Developing Adsorption Filters for Fluoride and Arsenic Removal from Water

By Simona Dossi

April 2018

Academic Supervisor: Dr. Enzo Mangano

Industrial Supervisor: Mr. Aaron Krupp

Abstract

This report presents the experimental work conducted during a six months Engineers without Borders UK placement in effort to progress Caminos de Agua's design of an adsorption filter in San Miguel de Allende, Mexico. The filter design's objective is to reduce local groundwater concentrations below the World Health Organisation's potable water limits of 10 μg/L and 1.5 mg/L, arsenic and fluoride respectively. Through batch experiments, Bayoxide ® E33 was concluded to be the most effective commercial arsenic adsorbent for the local groundwater over Bayoxide ® E33 HC and TiO_2 particles suspended in sand. Fixed bed and batch experiments, using Caminos de Agua's internally produced bone char fluoride adsorbent, investigated adsorption capacity and bone char production optimisation. The bone char's adsorption capacity was found to be independent of pyrolysis time, in a fixed bed system the adsorption capacity tested as 5.5 ± 0.3 mg/g for fluoride, acetic acid treated bone char performed with a 12 % higher adsorption capacity than untreated bone char, and an investigation of fixed bed system performance under varying solute flowrates was completed. Recommendations regarding improvement possibilities for future experiments conclude the report.

Table of Contents

i. Nomenclature

Notations

Symbol	*Name*	*Units*
a	Empirical constant	$[kg/m^3)/(kg/m)]^{-n}$
A	Area	$[m^2]$
c_i	Concentration of adsorbate solute	$[mol/m^3]$
c_i^s	adsorbate concentration at adsorbent surface	$[mol/m^3]$
d_p	Average particle diameter	$[m]$
J_i	Diffusion flux	$[mol/m^2s]$
J_{pi}	Pore diffusion flux	$[mol/m^2s]$
k_f	mass transfer coefficient	$[m/s]$
L	Bed length	$[m]$
m_{ad}	Adsorbent solid mass	$[g]$
n_i	Number of moles	$[mol]$
N_i	Mass transfer flux between adsorbent and bulk fluid	$[mol/sm^2]$
p_i	Partial pressure	$[Pa]$
P_i^{ref}	Standard state reference pressure	$[Pa]$
q_t	Specific adsorption capacity	$[mol/kg]$
Q_t	Volumetric flowrate	$[L/hr]$
r	Distance between the centres of the two isolated and interactive molecules	$[m]$
R	Ideal gas constant	$[J/Kmol]$
Re	Reynolds number	/
t	Time passed	$[hr]$
T	Temperature	$[K]$
u_s	Superficial fluid velocity	$[g/s]$
V	volume	$[m^3]$
x_i	mole fraction	/
Greek Letters		
$\boldsymbol{\epsilon}$	Potential well depth	$[m]$
$\boldsymbol{\sigma}$	Distance where the potential is equal to zero	$[m]$
$\emptyset$	Overall potential	$[J/mol]$
$\boldsymbol{\lambda_i}$	Isosteric heat of adsorption for component i	$[Jk/mol]$
$\boldsymbol{\mu_i}$	Chemical potential of component i	$[J/mol]$
$\boldsymbol{\mathcal{D}_i}$	Diffusivity for component i	$[m^2/s]$
$\boldsymbol{\mathcal{D}_{pi}}$	Pore diffusivity of component I	$[m^2/s]$
$\boldsymbol{\varepsilon_p}$	Adsorbent porosity	/
$\boldsymbol{\tau_p}$	Tortuosity	/
$\boldsymbol{\Delta p}$	Pressure drop	$[Pa]$
$\boldsymbol{\rho}$	T fluid density	$[kg/m^3]$
$\boldsymbol{\mu}$	Fluid viscosity	$[kg/ms^2]$,
$\boldsymbol{\pi}$	Spreading pressure	$[Pa]$

γ_i	The adsorbed-phase activity coefficient	/
ε_b	Bed void fraction	/
Subscripts		
ad	Adsorbent	
b	Fixed bed	
D	Attractive	
i	Component i	
LJ	Lennard jones	
p	Pore	
P	Polarisation	
Q	Gradient-quadrupole	
R	Repulsive	
S	Sorbate-sorbate	
s	Superficial	
t	At time t	
0	At time 0	
Acronyms		
BC	Bone Char	
DI	Deionised	
EWB-UK	Engineers with Borders UK	
HAP	Hydroxyapatite	
IAST	Ideal Adsorbed Solution Theory	
LES	Length Equivalent Equilibrium Section	
LUB	Length of Unused Bed	
MTZ	Mass Transfer Zone	
NGO	Non-Governmental Organisation	
TDS	Total Dissolved Solids	
TO	Treatment Objective	
TLUD	Top-Lit-Updraft	
WASH	Water, Sanitation, and Hygiene	
WHO	World Health Organisation	

ii. List of Figures

iii. List of Tables

Introduction

This technical report presents and analyses the experimental work conducted working within Caminos de Agua as an Engineers without Borders UK (EWB-UK) volunteer. The project work consists of experimental investigations regarding an aqueous arsenic and fluoride adsorption filter design. This introductory section will introduce the two organisations involved in the project, the project aims, and the context of the work within Caminos de Agua's previous contributions to the project.

1.1 Engineers without Borders UK and Caminos de Agua

EWB-UK is a nongovernmental organisation (NGO), which provides engineering expertise to projects in the developing world and inspires global responsibility within the engineering sector. EWB-UK believe that engineering should provide solutions for people in need of safe and healthy living environments regardless of income, nationality, or gender (Engineers without Borders UK, 2017). As well as running national educational projects, EWB-UK provides qualified engineer volunteers to non-profit organisations around the world. Volunteers assist projects which range from cook stove design to wind turbine implementation; all projects are divided within three engineering sectors: i. clean energy, ii. built environment, and iii. water, sanitation and hygiene (WASH) (Engineers without Borders UK, 2017). The work presented in this report summarises a EWB-UK WASH placement completed within Caminos de Agua between June and December 2017.

Caminos de Agua is an accredited NGO founded and based in San Miguel de Allende, Mexico. Caminos de Agua has collaborated with five EWB-UK volunteers including myself on the filter project; the project design decisions and work completed prior to the scope covered in this report are summarised in Section 1.3. Caminos de Agua's mission is to aid the water quality and scarcity crisis "for at-risk communities on [the] Independence Aquifer in Central Mexico" (Caminos de Agua, 2018); the aquifer is an underground water reservoir and the source of 99% of water usage for over half a million local residents (Caminos de Agua, 2018). The water level of the aquifer has been rapidly decreasing since the 1950s, thus endangering the availability and quality of its water (Caminos de Agua, 2018). Arsenic and fluoride concentrations above the World Health Organisation (WHO) potable limits have been recorded in water wells in the region; Figure 1, indicates the wells' general geographical locations and the well water's arsenic and fluoride concentrations relative to the WHO limits (Caminos de Agua, 2018; Targetmap, 2018). Part of Caminos de Agua's efforts to combat this issue consist in investigating functionalised bio-chars to develop low cost, sustainable, adsorption filters to treat the contaminated groundwater; this report presents contributions to this project.

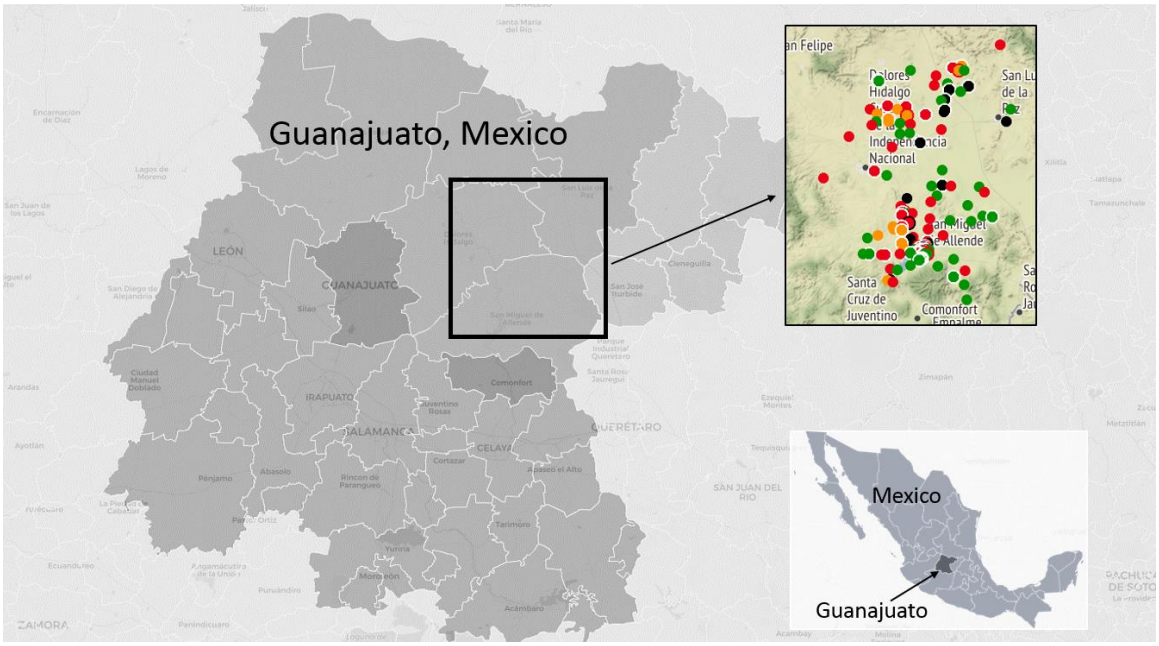

Well Water Arsenic and Fluoride Concentrations

- – Both contaminants concentrations below WHO potable limits
- – At least one contaminant concentration over ≤ 60% of WHO limit
- – At least one contaminant concentration over > 60% of WHO limit
- – At least one contaminant concentration over > 100% of WHO limit

Figure 1: Independence Aquifer well general geographic location and quality

1.2 Project Mission

The final objective of the project is to design and implement adsorption filters in communities throughout the San Miguel municipality to reduce well water concentrations of arsenic and fluoride to below the WHO potable limits: 10 μg/L and 1.5 mg/L respectively (World Helath Organisation, 2008). The feed water concentrations used for experiments are 40 μg/L of arsenic and 8.5 mg/L of fluoride because these values match or exceed, up to the 90th percentile of monitored wells' contaminant concentrations (Caminos de Agua, 2018). Caminos de Agua calculated the necessary volume of potable water for an average family of five for cooking and drinking as 25.2 litres per day, thus defining the specific filter capacity. Lastly, the filter needs to be accessible and practical for implementation in isolated rural communities. Adsorption was the separation process chosen due to the local and inexpensive fluoride adsorbent production; more information on process selection is presented in Section 3.1. All filter design objectives are summarised in Table 1.

Table 1: Design requirements for adsorption filter design

Adsorbent/s	▪ Locally sourced/produced ▪ Low cost
Capacity	▪ Flowrate:

	25.2 L/day for decentralised family-size filter
Feed Water	▪ Fluoride Concentration : 8.5 mg/L ▪ Arsenic Concentration : 40 μg/L
Treatment Objective	▪ Fluoride Concentration ≤ 1.5 mg/L ▪ Arsenic Concentration ≤ 10 μg/L
Energy/Power	▪ No Energy/Power input ▪ Operation Conditions: Temperature – ambient Pressure – no set objective

1.3 Context of Project within Caminos de Agua

Caminos de Agua had developed research regarding the adsorbents and the filter design; this section briefly summarises the relevant research completed and design decisions made before the commencement of my placement.

1.3.1 Fluoride Adsorbent Production

Caminos de Agua internally produces the bone char (BC) fluoride adsorbent. The production process consists in charring local butchers' waste bones pieces in a low-tech gasifier, built out of metal barrels as is shown in Figure 2, through pyrolysis. Heating biomass in the 400 - 1000 °C temperature range removes tars and oils from the biomass, thus producing carbon-rich, amorphous, and hydrophobic material (Kearns, 2012). Biochar is similar to activated carbon in terms of porosity and surface area (Kearns, 2012). Varying kiln designs and production processes were tested and improved; Figure 2 is an annotated illustration of the mechanisms within the top-lit-updraft (TLUD) biomass gasifier used to produce standard Caminos de Agua's fluoride BC adsorbent (Eikelboom, 2017). The gasified is made up of a 200 L reactor body, a 200 L combustion zone, and a chimney; the reactor body and combustion zone are labeled in left image in Figure 2. While the reactor body is filled with pieces of bones cut to be roughly the same sizes, the combustion zone is always left empty. When the biomass is ignited from the top of the reactor body, air enters the gasifier, thus introducing oxygen which results in combustion. The heat produces flammable gasses from the biomass which rise and burn with the inflowing secondary air in the combustion chamber; simultaneously, the flame front in the reactor body moves downwards as it burns the biomass and produces biochar. Variables influencing char quality (structure and properties) include burning time, average temperature (Kearns, 2012); experiment 4.1.1, presented in section 4.1.1 of this report, investigated the affect of burning time on final BC adsorption capacity. Results from early BC adsorption capacity investigations indicated that acid treating BC increased the material's fluoride adsorption capacity (Hobson & Terrel, 2015). Experiment 4.2.1, see Section 4.2.1, further investigated acid treatment effects by comparing untreated and acid treated BC adsorbent performance in fixed beds.

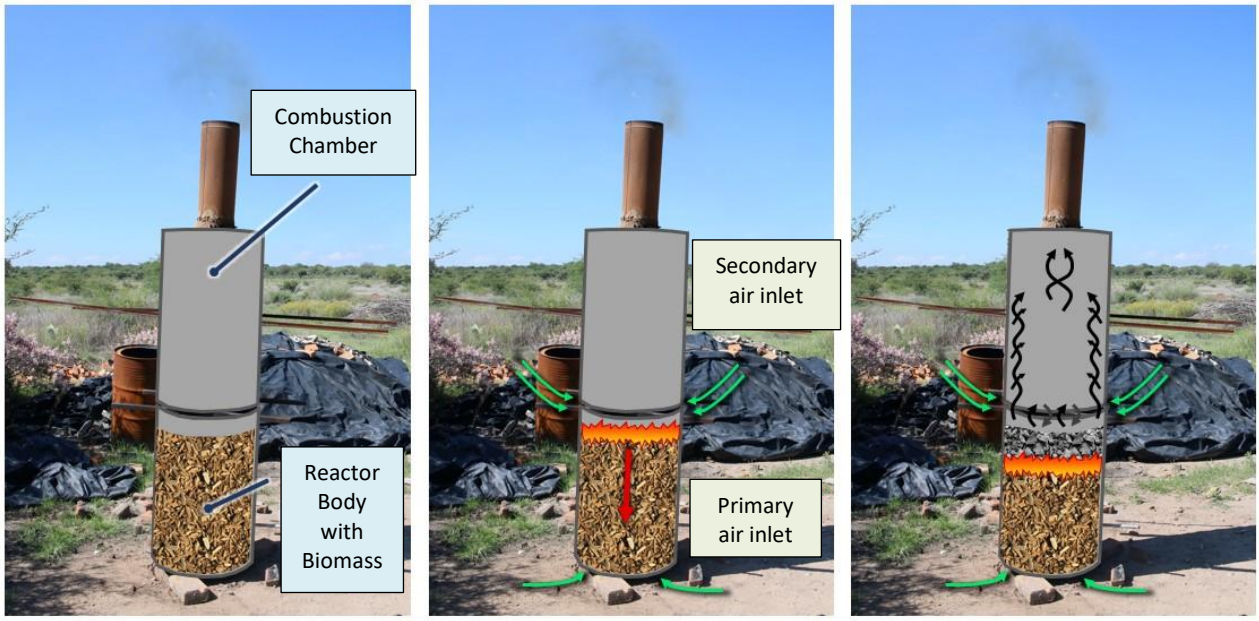

Figure 2: Finalised BC gasifier design with pyrolysis process illustration

1.3.2 Arsenic Adsorbent Production

A previous Caminos de Agua volunteer completed thesis research aimed at developing low-cost filter medium for groundwater arsenic removal (Eikelboom, 2017). Eikelboom produced and activated wood-char to produce ferrous granular materials, which have chemical affinity to aqueous arsenic and, therefore, are promising adsorbents . Using the same gasifier introduced in Section 1.3.1, shown in Figure 2, significant progress was made in developing adsorbents including wood-char, wood-char impregnated with Fe_2O_3, iron coated sand, and $FeCl_3$ impregnated wood-char (Eikelboom, 2017). Eikelboom's results after kinetic batch tests of the adsorbent concluded the commercial adsorbent Bayoxide ® E33 tested with the significantly highest adsorption capacity; 290.6 µg/g in contrast to the second highest adsorption capacity of 55.5 µg/g (Eikelboom, 2017). Due to these results, experiments 4.1.2 and 4.1.3 are aimed at comparing Bayoxide ® E33 with two other similar commercial adsorbents: Bayoxide ® E33 HC and a granular TiO_2 material mixed with sand. More information on the adsorbents used for the experiments presented is discussed in Section 3.3.

1.3.3 Lead Lag Design

The 'lead lag' design refers to the two columns in series process set up which is applied in all column experiments presented, and will be applied to the final filter design; refer to Section 3.5 for individual experimental set ups. The upstream column is referred to as the lead column, and the downstream column as the lag column. This design set up is adopted to maximise adsorbent use while maintaining outlet water concentrations below the treatment objective (TO), 10 µg/L and 1.5 mg/L arsenic and fluoride concentrations respectively. A single column outlet breaks through the TO when roughly 45 % of the fluoride saturation capacity has been adsorbed onto the BC in an

experimental column; therefore, leaving roughly 65 % of unsaturated adsorbent left unused. Two columns in series allow the upstream column to saturate fully while the downstream column maintains the system outlet concentration below the TO. Once the upstream column is saturated, it is disposed of or regenerated; the downstream, lag, column is then moved upstream, and a new, unsaturated, column is introduced in the downstream position. This cyclical regenerative approach ensures the system outlet is continually below the TO without wasting unsaturated adsorbent (Caminos de Agua, 2017). The lead-lag set up is schematically illustrated by Figure 3 (Caminos de Agua, 2017).

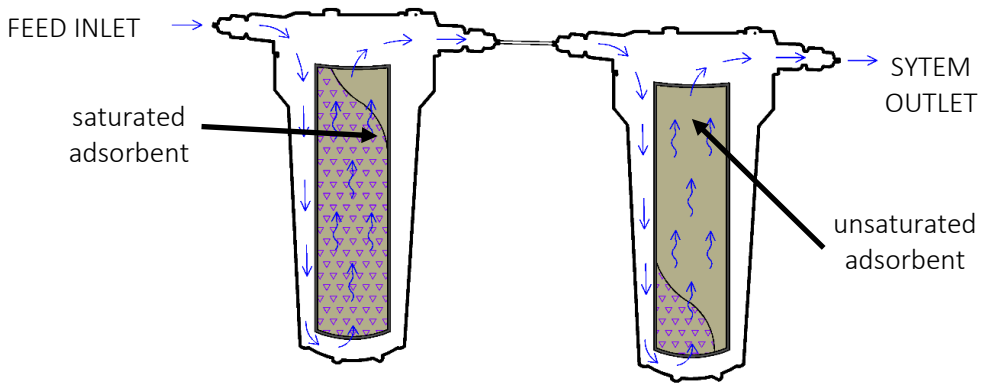

Figure 3: Lead lag design schematic illustration

1.4 Structure of Report

Section 1 has introduced the project's aims and its organisational and cultural context. Section 2 summarises relevant theoretical information on adsorption separation; it includes a comparison between adsorption and other suitable separation methods, a brief review of transport, kinetic, and equilibrium processes within adsorption, and a concise aqueous fluoride and arsenic adsorption literature review. Experimental objectives, equipment, and methodologies are outlined in Section 3, the experimental section. Section 4 presents all experimental results, alongside relevant data and analysis for each individual experiment. The results are discussed along with recommendations for future experiments in Section 5, the critical review. Lastly, the project and its results are summarised in Section 6, the conclusion. Detailed methodologies and further information regarding the project is available in the appendices.

2. Background and Theory

This section summarises relevant aspects of adsorption theory; it focuses on the governing dynamics of adsorption and adsorption batch and fixed bed systems, thus defining important theoretical basis for experimental analysis. The theory presented

assumes isothermal conditions and provides a general overview of the most significant theoretical aspects of adsorption rather than rigorous analytical models.

2.1 Separation Process Selection

A number of effective fluoride and arsenic removal processes have proved successful in water purification; the processes include ion exchange, adsorption, membrane process, and chemical addition (Chibi & Haarhoff, 2000). As outlined in Table 1, specific design constraints apply to Guanajuato's water crisis; these constraints dictated process selection. Ion Exchange, membrane processes, and chemical precipitation are unsuitable processes due to high capital, operational, and maintenance costs compared to adsorption, as well as the need for skilled operators. The most widely used separation methods for aqueous fluoride and arsenic removal are presented in Table 2 to illustrate adsorption filter systems are most suitable for the rural demand in question (Chibi & Haarhoff, 2000).

Table 2: Fluoride and arsenic water separation processes

Separation Process	Brief Description and Suitability
Ion Exchange	Synthetic ion exchange materials are produced to release ions in exchange of specific ions in solution (e.g: fluoride or arsenic). More expensive and specific separation material needed, compared to adsorption (Chibi & Haarhoff, 2000).
Adsorption	Porous material is produced and activated to adsorb aqueous contaminants through surface interactions. Low cost adsorbent materials and simple effective design can limit operational and capital costs significantly (Chibi & Haarhoff, 2000). Adsorption is also the process preference for liquid separation involving azeotropes, low relative volatilities, and smaller operation scales (Matthews, et al., 1983).
Membrane Processes	Reverse Osmosis membranes successfully remove ionic contaminants by pressurizing contaminated water through a semi-permeable membrane. Pressure requirements are set above osmotic press, therefore significant energy inputs compared to other separation processes are necessary (Chibi & Haarhoff, 2000).
Chemical Precipitation	Chemical addition can cause contaminant precipitation and reduction, thus allowing removal from aqueous systems. This process includes a sludge disposal problem and chemical addition which introduces complexity and a safety hazard to water quality (Chibi & Haarhoff, 2000).

2.2 Adsorption Theory

Adsorption is a chemical separation process; it consists of adhesion of a liquid, gas, or dissolved solid component (adsorbate) to the surface of a, usually solid, material

(adsorbent) (Ruthven, 1984). Adsorption processes are classified between physical adsorption and chemisorption. Physical adsorption only involves weak intermolecular forces (including van der Waals forces, and possibly electrostatic interactions) between the adsorbate and adsorbent; chemical bonds, on the other hand, bind the compounds in chemisorption (Ruthven, 1984). The most common differences between the types of adsorption processes are summarised in Table 3.

Table 3: Physical adsorption and chemisorption typical characteristics

Physical Adsorption	Chemisorption
Low enthalpy	High enthalpy
Non-specific	Highly specific
Multi-layer adsorption	Monolayer adsorption
Rapid process	Slow process
No electron transfer present	Electron transfer/Bond formation present

2.1.1 Forces and Energetics

In physical adsorption, as mentioned above, the interactions enabling separation are van der Waals forces and electrostatic interactions; electrostatic interactions are especially significant if the adsorbent has an ionic structure. Both aqueous fluoride and arsenic are charged ions and adsorbents tested have a surface charge; section 2.3 offers a more information on these specific adsorbent and adsorbate interactions. Van der Waals forces are also called dispersion-repulsion energy; dispersion forces are always present and can dictate equilibrium behaviour if stronger forces are not acting on the system. The dispersion-repulsion energy between two isolated interactive molecules, neglecting the non-dominant attractive terms and higher contributions to dispersion, is described through the Lennard-Jones potential function (Ruthven, 1984). Equation 1 illustrates the function: a combination of inverse sixth-power attractive term and inverse twelfth power repulsion term (Ruthven, 1984). The equation is illustrated graphically in Figure 4.

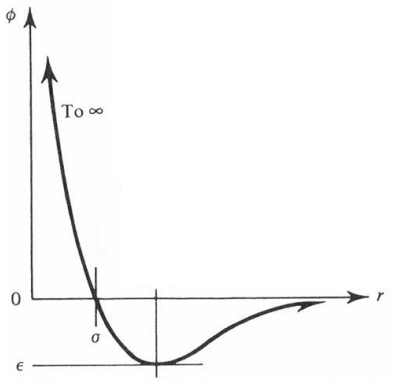

Figure 4: Lennard Jones Potential Mathematical Illustration

$$\emptyset_{LJ} = 4\epsilon[\left(\frac{\sigma}{r}\right)^{12} - \left(\frac{\sigma}{r}\right)^{6}] \qquad \textit{Equation 1}$$

Where r is the distance between the centres of the two isolated and interactive molecules in [m], ϵ is the potential well depth in [m], and σ is distance where the potential is equal to zero in [m].

In systems with a significant electric field present, electrostatic energies contribute to the energy of adsorption. Electrostatic energies may be caused by polarization, field-dipole, and field gradient-quadrupole interactions (Ruthven, 1984). In the case of aqueous fluoride and arsenic adsorption, charged ions dissolved in a polar adsorbate are adsorbing onto a charged surface adsorbent. A significant electrostatic energy contribution is, therefore, assumed for the system. Overall potential for an ionic adsorbent can be defined as the sum of the six contributor energies, as shown in Equation 2 (Ruthven, 1984). For chemisorption, the bond formation energies will significantly contribute to the overall potential.

$$\emptyset = \emptyset_D + \emptyset_R + \emptyset_P + \emptyset_\mu + \emptyset_Q + \emptyset_s \qquad \textit{Equation 2}$$

Where $\emptyset$ is the overall surface potential, $\emptyset_D$ is attractive potential, $\emptyset_R$is the repulsive potential, $\emptyset_P$is the polarisation contribution, $\emptyset_\mu$is the filed-dipole contribution, $\emptyset_Q$ is the field gradient-quadrupole interaction contribution, and $\emptyset_s$is the sorbate-sorbate interaction contribution, all in [J/mol].

In liquid adsorption, the point of zero charge can significantly affect the electrostatic interactions between adsorbate and adsorbent surface. The surface charge of natural particles, as is the case for the BC adsorbent, is contributed to the following three operational categories i. structural, ii. adsorbed proton, and iii. adsorbed ions; the point of zero charge is the pH value for which one contribution to surface charge equals zero at a given temperature, pressure and aqueous solution concentration (Sposito, 1998). Depending on the charge of the adsorbate components, a solution of pH below or above the point of zero charge can either hinder or favour adsorption.

The isosteric heat of adsorption is calculated through the Clausius-Clapeyron relation given in Equation 3. Note that equations containing partial pressure variables are suitable for gas adsorption systems but can be extended to liquid systems by expressing partial pressure in terms of concentration by assuming ideality (Perry & Green, 2008).

$$\lambda_i = RT^2 \frac{\partial lnp_i}{\partial T}_{n_i, n_j} \qquad \textit{Equation 3}$$

Where λ_i is the isosteric heat of adsorption for component i in [JK/mol], R is the gas constant in [J/Kmol], T is temperature in [K], p_i is partial pressure for component i in [Pa], and n_i is number of adsorbed moles of component i in [mol].

2.1.2 Sorption Equilibrium

Sorption equilibrium refers to the equilibrium between the adsorbate fluid phase and adsorbate-rich solid phase (Perry & Green, 2008). Equilibrium adsorption processes are characterised by adsorption isotherms; defined as amount of adsorbate bound to adsorbent surface, as a function of either pressure (for gas phase adsorption) or of concentration (for liquid phase adsorption) at constant temperature; single-component physical gas adsorption is the most investigated adsorption type in literature.

Experiments and molecular simulations can measure and describe various adsorption isotherm types; the most widely used IUPAC classification of adsorption isotherms is illustrated in Figure 5 (Donohue & Aranovich, 1998). Each isotherm class corresponds to a different adsorption system characteristic. Generally, type I isotherms are characterised by systems with a definite saturation limit (often occurring when pore diameter is similar to adsorbate molecular size) (Ruthven, 1984). Type II and III often describe systems with a variety of pore sizes range, type IV often is exhibited by systems that form two adsorbate molecules surface layers, and type V describes systems with strong intermolecular attraction effects (Ruthven, 1984).

The simplest equilibrium relationship for single-component systems is the linear (or Henry) isotherm; the most common and widely used isotherm models are the Langmuir, and Freundlich models (Perry & Green, 2008). A number of additional mathematical isotherm expressions, for both single and multi-component adsorption, are available in literature.

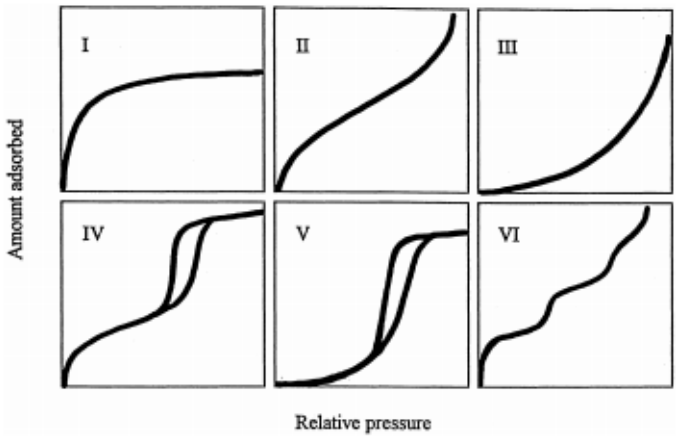

Figure 5: IUPAC classification of adsorption isotherm for gas-solid equilibria

Due to the complexity and expenses of modelling and testing multicomponent systems, estimations based on single component systems using molecular simulations and the Ideal Adsorbed Solution Theory (IAST) have been investigated extensively.

The IAST is a thermodynamic approach used to predict multicomponent adsorption. The theory relies on the belief that a component's partial pressure can be calculated by the product of its mole fraction and the pressure its pure component would apply at the same temperature and spreading pressure of the multicomponent mixture (as shown mathematically in Equation 5, when taking Υ_i as 1 due to the ideality assumption); this assumption is based on the Gibbs adsorption theory, stated in Equation 4 (Perry & Green, 2008). Although initially derived for gas systems, the theory was extended to dilute liquid mixtures with the following assumptions: a. the liquid solution is dilute, b. the adsorbed phase is an ideal solution, c. the adsorbent is thermodynamically inert, and d. the available surface area for all solutes is equal (Radke and Prausnitz, 1972).

$$Ad\pi = \sum_i q_i d\mu_i \qquad \textit{Equation 4}$$

$$p_i = \gamma_i x_i P_i^{ref}(T, \pi) \qquad \textit{Equation 5}$$

Where A is the area in [m^2], π is the thermodynamic spreading pressure in [N/m], μ_i is the chemical potential of component i in [J/mol], γ_i is the adsorbed-phase activity coefficient , $x_i$is component i mole fraction, $q_i$is the specific adsorbed amount in [mol/kg], and P_i^{ref} is the standard state in [Pa]

2.1.4 Transport

Section 2.1.4 aims to provide a mostly qualitative physical explanation of the governing mass transfer phenomena in adsorption systems. Extensive transport modelling efforts, however, are available in literature, especially for gas systems; for an extensive adsorption kinetic literature for activated carbon refer to *Adsorption: Science and Technology* (Rodrigues, et al, 1988).Transport within a bed packed with porous adsorbent, varies due to the nature and location of each transport mechanism. Figure 6 illustrates the different regions and types of transport that occur; they are categorised between intraparticle transport: pore diffusion, solid diffusion, reaction kinetics on adsorbent surface, and extraparticle transport and dispersion: external mass transfer, and fluid mixing (Perry & Green, 2008). Depending on the system, one or more of these processes limit the overall transport rate. In adsorption and desorption, the rate is usually limited by the transport inside porous media rather than kinetic sorption rates at the active sites (Ruthven, 1984).

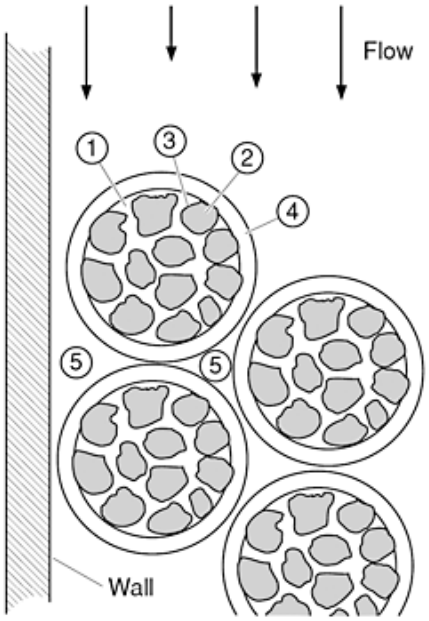

1. *Pore diffusion*- diffusion in liquid within pores

2. *Solid diffusion*- diffusion in adsorbed phase in micropores small enough that molecules do not escape surface force

3. *Reaction kinetics* at phase boundary

4. *External mass transfer* – bulk fluid to particle surface

5. *Fluid mixing* and flow through a fixed bed in fixed bed systems

Figure 6: General illustration of transfer locations in porous packed bed

Intraparticle transport is assumed to be a diffusive process described by Fick's Law which, for component i, is given in Equation 6 (Perry & Green, 2008). This law states that, for ideal systems, diffusivity is only dependent on the concentration gradient and is

independent of concentration. In real systems the driving force is the chemical potential gradient. Most transport models are based on this assumption, and on Fickian diffusivity (Perry & Green, 2008).

$$J_i = -\mathcal{D}_i \frac{\partial c_i}{\partial x_i} \qquad \textit{Equation 6}$$

Where J_i is the diffusion flux in [mol/m^{2}s], c_i is the adsorbate concentration, and $\mathcal{D}_i$is the diffusivity in [m^2/s], all for component i.

1. *Pore Diffusion*

Diffusion within pores is considered a diffusive process because there is either no, or very slow flow inside material pores (Ruthven, 1984). This mass transfer may be described by a combination of four different mechanisms depending on system conditions: a. Knudsen diffusion, b. an additional equivalent viscous contribution to diffusive flux, c. an additional molecular diffusivity contribution to diffusive flux, d. an additional molecular diffusivity contribution to diffusive flux, or d. surface diffusion. Knudsen diffusion dominates systems where the molecules' mean free path length is larger than the average pore diameter. Equivalent viscous contributions are significant when the system experiences a pressure gradient, while molecular diffusivity contributions are significant when a mixture is present in the system. Surface diffusion, lastly, is the mechanism describing diffusion in the case the molecules move in the direction of pores in the adsorbed phase (Cunningham & Williams, 1980). Surface diffusion is usually significant in systems with weak adsorption forces and is not yet deeply understood (Perry & Green, 2008). The four mechanisms introduced above are joined as necessary by joining molecular and Knudsen as resistances in series, and then the resulting resistance in parallel to surface and viscous resistances (as shown by Figure 6 when taking the diffusion coefficients as the inverse of resistance) (Cunningham & Williams, 1980).

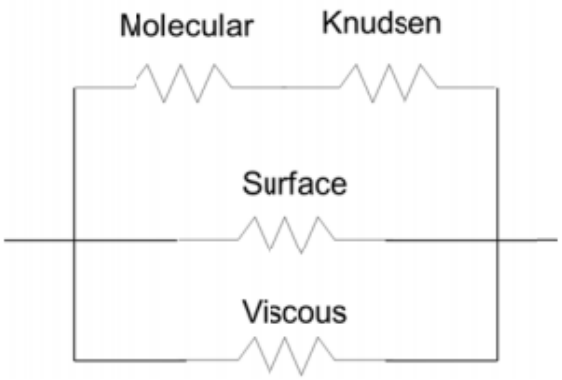

Figure 7: Schematic of pore diffusion resistances combination

Less rigorously, the diffusion flux through fluid-filled pores, can be described, as shown in Equation 7, in terms of the pore diffusion coefficient $\mathcal{D}_{\mathrm{pi}}$, which corrects the diffusion coefficient to account for diffusion path and variation pores diameter through the integration of the tortuosity factor, as shown in Equation 8. Experimental tortuosity factors, which correct for the deviating and length or pore paths, generally fall in the range 2 – 6 and decrease as the particle porosity increases (Perry & Green, 2008).

$$J_{pi} = -\varepsilon_p \mathcal{D}_{pi} \frac{\partial c_{pi}}{\partial z} \qquad \textit{Equation 7}$$

$$\mathcal{D}_{pi} = \mathcal{D}_i / \tau \qquad \textit{Equation 8}$$

Where J_{pi} is pore diffusion flux in [mol/m^{2}s], $\mathcal{D}_{pi}$ is the pore diffusivity in [m^2/s], ε_p is the adsorbent porosity, τ is the tortuosity, and z is the bed length direction in [m].

2. *Solid Diffusion*

Fick's transport diffusivity for solid, or micropore, diffusion is described by Equation 9. Correcting the driving force as the chemical potential is allowed by using the corrected diffusivity, $\mathcal{D}_{0i}$; Equation 10 shows how the corrected diffusivity is related to the diffusivity in Equation 9 through multiplication with the Darken correction factor.

$$J_i = -\mathcal{D}_i \frac{\partial q_i}{\partial z} \qquad \textit{Equation 9}$$

$$\mathcal{D}_i = \mathcal{D}_{0i} \frac{dln(p_i)}{dlin(q_i)} \qquad \textit{Equation 10}$$

Where $\mathcal{D}_{0i}$ is the corrected diffusivity in [m^2/s].

3. *Reaction Kinetics*

Rate equations describe interphase mass transfer in adsorption systems. Combining the general component balance for a chose particle geometry and the relevant flux expressions (depending on the limiting transport process in the system), produces rate equations that can be solved with appropriate boundary conditions (Perry & Green, 2008).

4. *External Mass Transfer*

Avoiding rigorous analysis of hydronamics around particles, mass transfer around the adsorbent can be straightforwardly described in terms of a mass transfer coefficient, available from correlations in terms of the Sherwood number and the Schmidt number. Packed bed correlations are available in Perry's Chemical Engineering Handbook (Perry & Green, 2008). The mass transfer flux on particle surface is generally described by Equation 11.

$$N_i = k_f (c_i - c_i^s) \qquad \textit{Equation 11}$$

Where $N_i$is the mass transfer flux between the adsorbent and bulk fluid in [mol/sm^2], k_f is the mass transfer coefficient in [m/s], c_i is the adsorbate bulk fluid concentration in [mol/m^3], and c_i^s is the adsorbate concentration at the adsorbent surface [mol/m^3].

5. *Fluid Mixing and Flow through a Fixed Bed*

When considering the bulk fluid flow in packed beds, the most important parameter is the pressure drop resulting from fluid flowing at a particular flowrate. The Ergun Equation for a packed bed, given by Equation 12, is the mathematical description of flow for a single incompressible fluid through an incompressible bed of granular solids. (Perry & Green, 2008). The Reynolds number and the bed void fraction equations necessary for the Ergun Equation are given by Equation 13 and Equation 14 respectively. At low Reynolds number the viscous forces dominate therefore the 1.75 component in the

Ergun Equation becomes insignificant and pressure drop is proportional to bed void fraction, fluid viscosity and superstitial velocity (Perry & Green, 2008).

$$\left(\frac{\Delta p}{L}\right)\left(\frac{d}{\rho u_s^2}\right)\left(\frac{\varepsilon_b^3}{1-\varepsilon_b}\right) = \frac{150}{Re} + 1.75 \qquad \textit{Equation 12}$$

$$Re = \frac{d u_s \rho}{(1-\varepsilon_b)\mu} \qquad \textit{Equation 13}$$

$$\varepsilon_b = (V_b - V_{ad})/V_b \qquad \textit{Equation 14}$$

Where Δp is the pressure drop in [Pa], L is the bed length in [m], d is the average particle diameter in [m], ρ is the fluid density in [kg/m^3], μ the fluid viscosity in [kg/ms^2], us is the superficial velocity in [g/s], ε_b is the bed void fraction, and Re the Reynolds number.

The dispersion coefficient in the axial dispersion term (present in the column mass continuity equation, which is found by substituting Equation 7 in Equation 17) takes into account all contributions to axial mixing in packed beds and is best determined experimentally but can be also estimated from relevant correlations. The axial dispersion term in the continuity equation is often assumed negligible but can be especially relevant for liquid flow in large beds (Perry & Green, 2008).

2.2 Adsorption Systems

2.2.1 Batch

Prediction modelling combines conservation equations and relevant rate equation for the appropriate system controlling mechanism. Different mathematical solutions are, therefore, solved for external mass-transfer control, solid diffusion control, pore diffusion control, and combined resistances. Section 3.2.1 is limited to provide non-rigorous mass conservation equations and the adsorption capacity calculation method assuming constant volume, well-mixed batch systems with uniform spherical adsorbent particles.

The batch conservation equation is expressed by Equation 15 (Loebenstein, 1962).

$$c_0 V = c_t V + q_t m_{ad} \qquad \textit{Equation 15}$$

Where c_0 is the concentration of adsorbate solute at initial time in [mol/L], c_t is the adsorbate solute concentration at time t in [mol/L], q_t is the adsorption capacity at time t in [mol/g], and m_{ad} in the adsorbent solid mass in [g].

The specific adsorbed amount at time *t*, or the adsorption capacity, mentioned above is calculated through rearrangement of Equation 15, and is expressed by Equation 16.

$$q_t = \frac{V(c_0 - c_t)}{m_{ad}} \qquad \textit{Equation 16}$$

2.2.2 Fixed Bed Columns

Fixed-bed systems are most widely used for adsorption separations; rigorous modelling of these systems involves complex dynamics and analysis. Design efforts are u based on adsorption equilibrium and dynamic character (Perry & Green, 2008). The two best-known classical analytical methods used for fixed-bed behaviour analysis are local equilibrium theory (which ignores all mass-transfer resistances and focuses on isotherm shape), and constant pattern analysis (which produces the maximum breadth to which a mass-transfer zone will spread) (Perry & Green, 2008). Section 3.2.2 will not discuss these methods but rather give an overview of fixed bed dynamics and breakthrough curves. Equation 18 gives the mass continuity equation for continuous fixed bed systems.

$$\varepsilon_b \frac{\partial J_i}{\partial z} + \varepsilon_b \frac{\partial c_i u}{\partial t} + \varepsilon_b \frac{\partial c_i}{\partial t} + (1 - \varepsilon_b) \frac{\partial q_i}{\partial t} = 0 \qquad \textit{Equation 17}$$

The breakthrough curve describes the adsorption behaviour of a fixed-bed column; it is formed by plotting the ratio of c_t/c_0 (outlet adsorbate solute concentration/feed adsorbate solute concentration) against time (Han, et al., 2009). The mass-transfer zone (MTZ) concept is used for many design predictions; Figure 8 shows two bed concentration profiles, illustrating the MTZ, equivalent equilibrium section (LES), and length of equivalent unused bed (LUB) zones. Upstream of MTZ, the adsorbent and feed are in equilibrium; within the MTZ, a drop in adsorbate concentration occurs. Downstream of the MTZ, the adsorbent is in its initial state. At the beginning of a bed's lifespan, the MTZ is closest to the bed inlet; c_t decreases to c_0 in an S-shaped curve concentration profile within the zone (Barros, et al., 2013). As more time passes, the bed is slowly saturated, starting with the region closest to the fluid inlet. When outlet concentration reaches the treatment objective, the system has broken through and the time taken for this is to occur is called the breakthrough time.

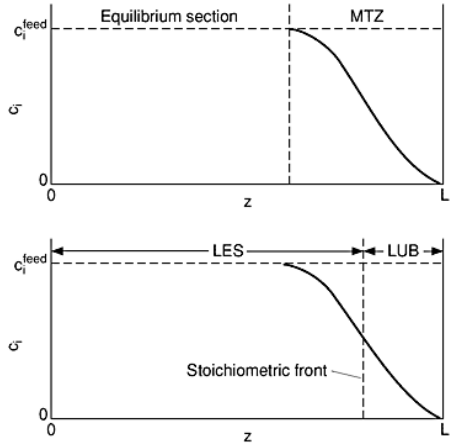

Figure 8: Schematic illustration - concentration profile in an adsorption fixed bed

The total adsorption capacity of the column (q_t) is calculated with Equation 18 for variable flowrates.

$$q_t = \frac{\int_{t_0}^{t} Q_t(c_0 - c)dt}{m_{ad}} \qquad \textit{Equation 18}$$

Where Q_t is the inlet flowrate at time t in [L/hr], and t is time passed in [hr].

2.3 Aqueous Arsenic and Fluoride Adsorption Literature Review

Lastly, section 2.3 will summarise significant literature on arsenic and fluoride adsorption in water solutions; focusing on adsorbents similar to those used in the experiments presented in this report. Fluoride ingestion may cause fluorosis, a disease affecting teeth and bones, to varying extents of severity depending on the amount and prolongation of ingestion (WHO, 2001).

2.3.1 Aqueous Fluoride Adsorption on BC

Fluoride removal from drinking water has been studied extensively; numerous publications in literature contain information on specific developed adsorbents as well as other, more expensive, removal techniques including ion exchange, chemical precipitation, and electrodialysis. This section focuses on literature published on BC removal of aqueous fluoride.

a. BC Characterisation

BC is produced through carbonisation of bones and contains roughly 10-25 % carbon, and 75-90 % hydroxyapatite (HAP), depending on carbonisation conditions and animal bone type (Medellin-Castillo & et.al., 2014). Calcite ($CaCO_3$) also has been found to make up roughly 10 % of BC (Medellin-Castillo, et al., 2007). The dominating mechanism of fluoride adsorption on calcium hydroxyapatite ($Ca_{10}(PO_4)_6(OH)_2$) has been characterised as electrostatic attractions and ion exchange (Fan, et al., 2003) (Sundaram, et al., 2008). Medellin-Castillo et al. experimentally proved that BC's adsorption of fluoride occurs due to HAP's presence by solving for adsorption capacity ratios of BC and HAP (q_{BC}/q_{HAP}) under various conditions; the ratio was always very close to HAP's weight fraction in BC (0.848) (Medellin-Castillo & et.al., 2014). BC particles are irregular, varied, fractured, porous, BC does not have a uniform particle radius distribution; specific numerical values for these parameters will also vary between batches (Medellin-Castillo & et.al., 2014). Medellin Castillo et al. tested for BC chemical stability by mixing BC with acidic and basic solutions at various pH and measuring Ca^{2+} and PO^{4-} concentrations in the solutions; their results, indicate that both the BC and the HAP dissolve drastically more in

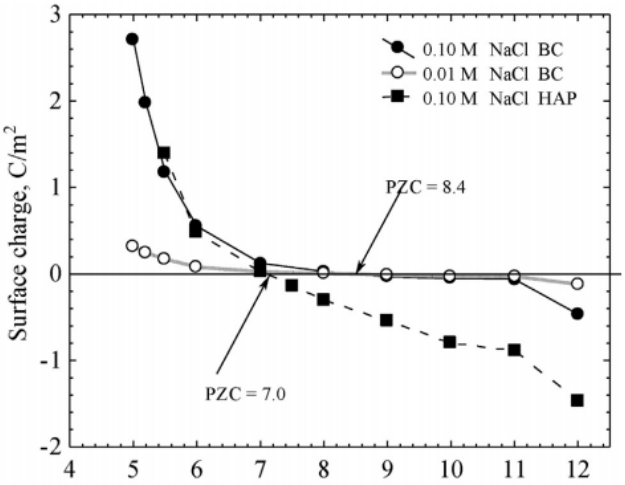

Figure 9: BC and HAP point of zero charge

solutions of pH < 4. Surface charge and point of zero charge of BC and HAP were also determined by Medellin Castillo et al. through titration; the result is given in Figure 9.

b. Adsorption Isotherm Equilibrium Data Fit

Experimental equilibrium data was successfully fit to the Freundlich, Langmuir, and Prausnitz-Radke isotherms with percentage deviations of 17.1, 16.9, and 10.5 % respectively (Medellin-Castillo & et.al., 2014).

c. BC Adsorption Capacity

i. pH and Temperature Dependence

Adsorption capacity of BC was experimentally characterised to perform at its maximum at a pH of 3 and decrease by a factor of 20 as pH was increased to 12, due to the electrostatic interactions between F^- ion and BC surface (Medellin-Castillo, et al., 2007). This pH dependence is explained by BC's positive charge below its point of zero charge (in solution with a pH of 8.4), therefore attracting more significantly the negative F^- ions. Furthermore, BC's adsorption capacity tested independent of temperature for temperatures between 15 and 35°C (Medellin-Castillo, et al., 2007).

ii. Competing Ions

In Medellin-Castillo's results, BC's fluoride adsorption capacity was reduced by the presence of competing ions in the drinking water of San Luis Potosi, Mexico. Ions Cl^-, NO^{2-}, NO^{3-}, CO_3^{2-}, HCO_3^-, and SO_4^{2-} are the most likely competing ions found in drinking water. Medellin-Castillo et al. ranked BC anion affinity as: $F^- > Cl^- > CO_3^{2-} > NO^{2-} \approx NO^{3-} \approx HCO_3^- \approx SO_4^{2-}$. Competition will depend on specific water chemistry: specific ionic concentrations and water pH; equilibrium data for the ions mentioned, however, can be found in Medellin-Castillo et al.'s paper and used for suitable estimation.

2.3.2 Aqueous Arsenic Adsorption

a. Arsenic Chemical Occurrence

The most abundant species of inorganic arsenic in the aqueous environment are arsenite (As(III)), and arsenate (As(V)), often occurring as arsenous acid, arsenic acid, and their salts (Bissen & Frimmel, 2003). Furthermore, organisms methylate inorganic arsenic compounds to form organic compounds including monomethylarsonic acid (MMA), and dimethyl-arsinic acid (DMA) (Bissen & Frimmel, 2003). Sources of arsenic in the environment range from natural (arsenic is present in over 245 minerals) to human-caused (including industrial waste disposal and burning of fossil fuels). Many arsenic compounds are toxic and both As (III) and As (V) limit the mitochondria's activities. As(III)'s strong affinity to sulfhydryl groups result in enzyme deactivation, and As (V) competes with phosphate and can therefore uncouple oxidative phosphorylation and harm adenosine triosphate's high energy bonds (Bissen & Frimmel, 2003).

b. Arsenic Oxidation Significance

As(V) removal is easier than As (III); oxidation As(III) to As(V) (given in Equation 19) is very slow in presence of air and pure oxygen (experiments cite limited percent of As(III)

oxidised after days of presence with air, better but still slow results are cited when purging solution with air or oxygen). Oxidation, however, can be accelerated through a variety of methods including addition of oxidants, catalytically in presence of activated carbon, or by manganese oxides (Bissen & Frimmel, 2003).

$$H_3AsO_4 + 2H^+ + 2e^- \rightarrow H_3AsO_3 + H_2O \qquad \textit{Equation 19}$$

Fixed bed adsorption filters have been developed and tested successfully in the developing world as an arsenic removal technique. Effective tested adsorbents are subdivided in categories of adsorbents containing iron compounds, zero valent ions, and activated alumina. Iron compounds containing adsorbents include granulated ferric hydroxide (GFH), which contains β-FeOOH, and Bayoxide® E33 which contains iron hydroxide (Bissen & Frimmel, 2003).

c. Bayoxide ® E33 Adsorption Capacity

Lin et al. published data regarding Bayoxide ® E33's adsorption of arsenic. Through temperature controlled batch reactions, kinetic and equilibrium arsenic adsorption was determined and successfully fit to the Freudlich isotherm mathematical expression given by Equation 20.

$$q_t = ac_t^{\frac{1}{b}} \qquad \textit{Equation 20}$$

a is an empirical constant in $(g/cm^3)/(g/cm^3)^{-n}$, b is an empirical constant

Equilibrium adsorption was tested at five different pH conditions, with four different initial concentrations. Adsorption capacity was strongly dependent on pH; as pH increased, adsorption on Bayoxide ® E33 decreased. For Bayoxide ® E33, the pH of point of zero charge was measured through titration as 8.6; therefore, for pH << 8.6, the adsorbent's surface will be mostly positively charged allowing more binding to negatively charged arsenate anions. Through the pore diffusion model combined with the Freundlich isotherm parameters, diffusion coefficients were calculated and kinetic adsorption curves were successfully predicted (Lin, et al., 2006).

3. Experimental

Section 3 provides experimental information. The section starts by providing an outline of experiments ran and individual experimental objectives, it proceeds to list all apparatus used with errors, and outline experimental methodology, finally it provides experimental design schematic diagrams.

3.1 Experiments Introduction and Objectives

3.1.1 Overall Project Quantitative Objective

The numerical adsorption filter requirements are based on the water volume required for drinking and cooking per person, and feed concentration exceeding 90 % of the

monitored wells in the region, due to variation in arsenic and fluoride concentrations amongst the wells; the requirements are summarised in Section 1.2, Table 1.

3.1.2 Experiments Outline

The approach selected for filter development within Caminos de Agua's Research and Technology team is divided in three stages; i. material selection and production, ii. adsorption capacity determination, and iii. regeneration investigation. These stages are designed as an iterative process, throughout which new data and information from experiments in one stage can inspire innovation and improvement in a previous or subsequent stage to ensure continuous design improvement. This section provides a list of all the experiments ran, which stage each belongs to, and a summary of their respective objectives. The experiments are numbered based on the subsection each experiment is presented in within Section 4. Note that experiments 4.2.1, 4.2.2, and 4.2.3 are the most significant experiments in terms of size, duration, investigated parameters, and system complexity and will therefore be discussed in more depth.

i. Material Selection and production

5.1.1 BC Burns - Varying Duration

Experiment Type: 24 hour kinetic test

Objective: Determine how charring process duration in gasifier affects adsorption capacity of BC – maintained between 400°C and 600°C for 1, 1.5, 2.5, 4, and 5.5 hours.

5.1.2 Commercial Arsenic Adsorbents

Experiment Type: 24 hour kinetic test

Objective: Compare adsorption capacity of selected commercially available aqueous arsenic adsorbents.

5.1.3 Commercial Arsenic Adsorbents

Experiment Type: 1 week kinetic batch experiment

Objective: Compare adsorption capacity of selected commercially available aqueous arsenic adsorbents.

ii. Adsorption Capacity Determination

5.2.1 Columns Experiment 1: Varying Adsorbent Preparation

Experiment Type: Fixed bed experiment

Objective: Model and monitor adsorption efficacy of untreated BC and acetic acid – treated BC adsorption of aqueous fluoride in continuously operated packed beds.

5.2.3 Columns Experiment 2: Varying Flowrate

Experiment Type: Fixed bed experiment

Objective: Investigate effect of varying flowrate on untreated BC adsorption of aqueous fluoride.

iii. Regeneration Investigation

5.2.2 Regeneration Experiment

Experiment Type: Fixed bed experiment

Objective: Investigate regeneration options of fluoride saturated BC with Reverse Osmosis treated water as a carrier.

3.2 Apparatus and Error

3.2.1 Water Testing and Sampling

a. Fluoride Testing

- Hach Colorimeter DR/850 (shown in Figure 10)
- Fluoride reagent: SPADNS2

Error: ±0.06 mg/L for undiluted samples; ± Dilution Factor × 0.06 mg/L for diluted samples**.** Dilution is necessary for samples of fluoride concentration above 2 mg/L.

Figure 10: Hach fluoride test colorimeter (Hach, 2017)

b. Arsenic Testing

- ITS QuickTest Field Arsenic Kit (shown in Figure 11)

Figure 11: ITS arsenic field test kit

Error: Results' errors vary with concentration of sample; refer to Table 4 for summary of errors.

Table 4: ITS arsenic field test kit errors

[As] *µg/L*	1-10	12-15	16-30	>30
Absolute error *µg/L*	0.5	1	2.5	5

Experiments only deal with arsenic concentration of or below 40 µg/L because that is the feed water arsenic concentration used; Table 4 therefore only shows errors of interest to experimental results. During the course of the placement, I conducted a series of tests to assess the accuracy of the ITS field arsenic test kit and Hach arsenic field test kit, which was also used by Caminos de Agua. This experiment is presented in an internal report given in Appendix D. The difficulties and complexities of testing very dilute aqueous concentrations of arsenic is further discussed and analysed in section 5.1.2.

- Pipette and disposable pipette tips

Error: ± 0.05 ml

- Sterile Sampling Bags

3.2.2 Batch Experiments

- Test Tube Containers – Capacity: 0.09 L
- Tumbler (shown in Figure 12)
- Three scales

For adsorbent weighing:

Error: ±0.0005 g

For flowrate monitoring:

Error: ±25 g

For water sample weighing:

Error: ±0.5 g

- Coffee Filter Paper

Figure 12: tumbler used for batch experiments

3.2.3 Column Experiments

Figure 13: Fixed bed experimental set up

- Column Beds – Capacity: 0.695 L
- PVC Piping valves, and tees
- Blue Storage Tank – Capacity: 80 L
- Outlet Water Tank – Capacity: 20 L

All column experimental equipment is shown in
Figure 13

- Timer

Error: ±0.5 s

- Volumetric cylinders

Error: ±0.0025 L

3.2.4 Error Calculation

The apparatus listed in sections 3.2.1-3.2.3 includes all experimental apparatus used for measurements. For all calculations and results obtained from experimental data, therefore, the apparatus error was calculated using Equation 21 and the appropriate propagation of error calculation.

$$rel_{\varepsilon}(x) = \frac{abs_{\varepsilon}(x)}{x} \qquad \textit{Equation 21}$$

Where $abs_{\varepsilon}(x)$ is the absolute experimental error exhibited by the measuring device use in the relevant units for the measurement, and $rel_{\varepsilon}(x)$ is the relative error.

3.3 Adsorbent Materials Tested

Five adsorbent materials were tested throughout the experiments. Adsorbents are first compared by their 24 hour kinetic test experiment performance, and subsequently are compared from the results of a week-long batch test. Finally, the most promising material is tested in the column set up in order to calculate its adsorption capacity in a continuous column system which most closely models the final filter design. Two differently treated BCs were tested for fluoride removal, and three different commercial adsorbents were tested for arsenic removal. As a reference for the rest of the report, Table 5 lists the adsorbent materials tested.

Adsorbent materials are classified as crystalline or amorphous materials and can be either hydrophilic or hydrophobic. All materials tested in this report are amorphous and hydrophobic. Surface area, pore size distribution, tortuosity, and surface charge are all adsorbent material parameters that affect adsorbent performance. Due to the limitations of sophistication of equipment available, such in-depth investigation of material parameters and related performance effect was not performed. With more advanced apparatus available, capillary condensation or mercury porosimetry could be used to characterise material pore distribution.

Table 5: Adsorbent materials tested

Name	*Adsorbate*	*Treatment/ Additional Information*
Untreated BC	Fluoride	▪ Charred through pyrolysis (see section 1.3.1 for an overview of Caminos de Agua's BC production, and Appendix A.1.1 for its methodology). ▪ Not that BC used in experiment 4.2.3 had been flushed with RO treated water (methodology provided in Appendix A.1.2) in order to remove phosphate which interferes with fluoride tests ▪ Varying pyrolysis time duration effect on adsorption capacity tested in experiment 4.1.1
Acid Treated BC	Fluoride	Treated with acetic acid (refer to Appendix A.1.3 for the treatment methodology)
Bayoxide ® E33	Arsenic	Commercial material: produced by AdEdge Technologies (AdEdge Technologies Inc., 2011)
TiO_2 granular media suspended in sand	Arsenic	Commercial material: produced by Aqua Clara (Hering, et al., 2017)
Bayoxide ® E33 HC	Arsenic	Commercial material: produced by Lanxess (Lanxess, 2018)

3.4 Methodology

Section 4.4 provides a brief methodology for each experiment and feed water preparation; detailed methodologies can be found in Appendix A.

3.4.1: Feed Water Preparation

Feed water used originated from a particular community well, for more information on the feed water chemistry refer to Appendix B. The water was stored in a 1 m^3 storage container unit, and mixed for 10 minutes with an electric drill; once mixed, samples from the top and the bottom of the storage tank were collected and tested. If the concentrations of the two samples were within 10 % of each other the water was considered well mixed, if not the mixing and testing was repeated until the samples' concentration variation was acceptable. Dilution calculations were performed to obtain the concentrations listed in Table 1 (40 μg/L of arsenic, and 1.5 mg/L of fluoride), and the necessary volume of tap water was added. The mixing and testing steps were repeated until the water was well mixed, and of the correct concentration.

3.4.2: 24 hour Kinetic Tests Methodology

Preparing BC Samples – this methodology applies to Experiment 4.1.1

The same batch of butcher bones was cut in pieces roughly 3-5 cm in length and divided in smaller sub-batches of roughly the same weight in empty metal paint cans; all the batches were placed in a gasifier with three thermocouples. While monitoring the temperature of the gasifier, batches are removed one by one, ensuring that the batches

are maintained between 400°C and 600°C for 1, 2.5, 4, and 5.5 hours respectively. The batches' fluoride adsorption capacities are then compared amongst each other and with a standard Caminos de Agua BC batch (produced by maintaining the bones above 400°C and below 600°C for 1.5 hours).

This methodology applies to experiments 4.1.1, and 4.1.2:
Adsorbent weights to be tested are chosen based on literature or cited adsorption capacity values. The adsorbent is weighted and placed in test tubes; two test tubes for each weight chosen are prepared to have doubles to verify results and control human error. Volume of well water of tested fluoride and arsenic concentration is measured and introduced to test tube using the pipette. All measurements are recorded. Test tubes are placed within test tube tumbler and left to tumble for 24 hours. After the necessary time has passed, the adsorbent is filtered out using coffee filter paper and the resulting concentration of water is tested and noted.

3.4.3: 1 Week Batch Test Methodology
This methodology applies to experiment 4.1.3:
Appropriate adsorbent weight for test tube water volume is chosen based on 24-hour kinetic test result. 22 test tubes are prepared, all with the same weight of adsorbent and 90 ml of feed water introduced with the pipette, as explained in Section 3.4.1. The adsorbent is filtered out, and concentration of water is measured, for two test tubes at a time after 0, 0.25, 0.5, 1, 1.5, 3, 6, 12, 24, 72, and 168 hours; thus, monitoring the adsorbent's performance on well water throughout a week long time period.

3.4.4: Column Experiments Methodology
This methodology applies to experiments 4.2.1, 4.2.2, and 4.2.3:
Water flows through system and is collected in storage container downstream of system. Every eight hours, sample bags are used to take manual samples at the sampling points after each individual column and from the feed water storage tank. At each sampling time, water collected downstream of system is weighted and thus the flowrate is calculated and adjusted if necessary. Sampled water concentration is tested and noted. For experiments 4.2.1 and 4.2.3, before starting experiment with feed water, reverse osmosis treated water is ran through columns, monitored and tested every eight hours. Experiments are continued until TO is broken through by system outlet. Section 3.5.2 provides more specific process control methodology referring to labelled set up schematic diagrams for each fixed bed experiment.

3.5 Experimental Design
Section 4.5 provides experimental design set up, and descriptions for all experiments ran. For capacities of equipment or experimental units please refer to section 4.2.

3.5.1 Batch Experimental Design
The following experimental design applies to experiments 4.1.1, 4.1.2, and 4.1.3:
A regular household fan was converted to a test tube tumbler. Fan blades were removed and replaced by a circular even piece of wood with 42 circular holes large

enough to hold the test tubes. At the beginning of dose and batch experiments, the fan motor is turned allowing the water and adsorbent materials to be constantly tumbled and all the water in the test tube to come in contact with the adsorbent material. A schematic illustration of the set up is provided by Figure 14, and a photograph by Figure 12. It is worth noting, that test tubes are positioned at varying distances from the centre of the tumbler (varying radiuses); this affects the angular velocity experienced by each test tube, thus introducing variation to the tumbling. Due to the consistency of experimental results, this variation does not seem to have significant impacts on the experimental results presented.

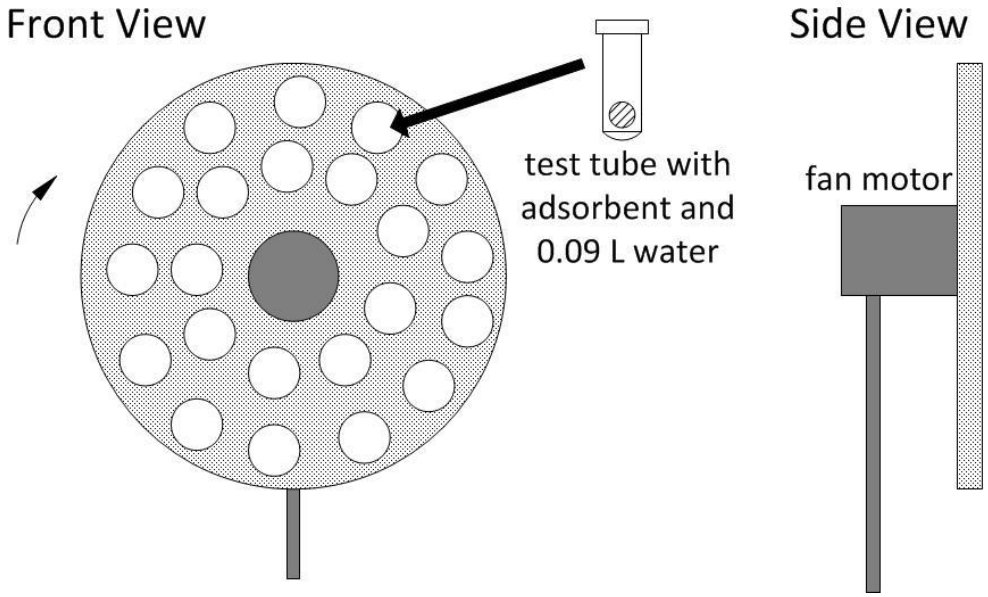

Figure 14: Batch and dose experiments schematic design

3.5.2 Fixed Bed Experimental Designs

Section 3.5.2 provides the experimental set up and description for all fixed bed experiments ran. The same equipment was used for all fixed bed experiments (4.2.1 - 4.2.3); the system parameters are summarised in Table 6: Fixed bed systems parameters. Water properties are assumed for fluid properties, average particle diameter is estimated based on sieve size used, and bed void fraction is calculated based on literature values for BC density (Chen, et al., 2008).

Table 6: Fixed bed systems parameters

Average particle diameter	1.285×10^{-3} m	Superstitial Fluid velocity [m/s]	
Bed void fraction	0.68	Experiment 4.2.1	7.97×10^{-4}
Bed cross sectional area	0.00037 m^2	Experiment 4.2.3	
Bed length	1.9 m	Set up 1	1.59×10^{-3}
Fluid density	1000 kg/m^3		
Fluid viscosity	0.00089 kg/ms^2	Set up 2	1.22×10^{-3}
BC mass in column	451 g		

a. Experiment 4.2.1

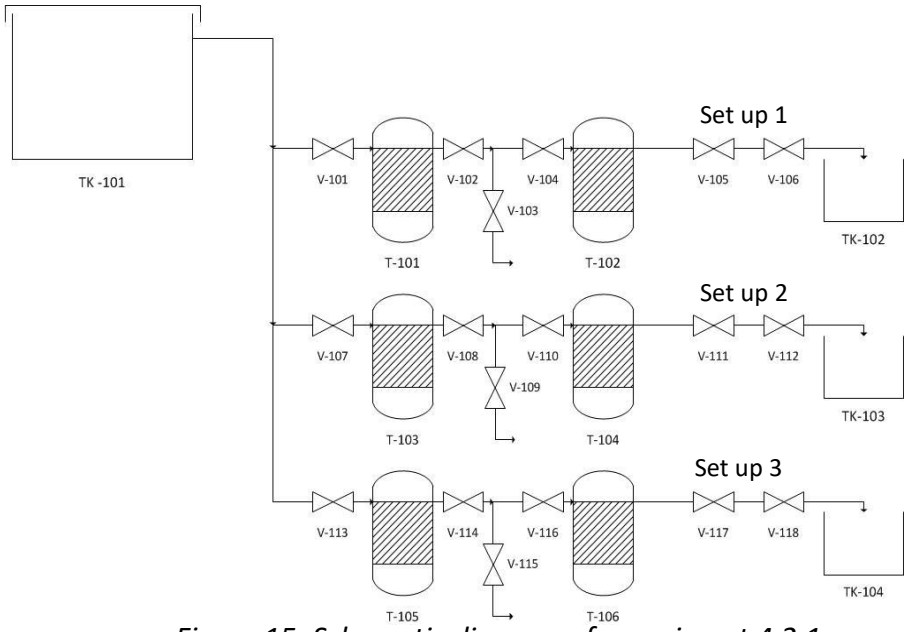

Figure 15: Schematic diagram of experiment 4.2.1

Three process lines consisting two fixed beds in series (T-101 – T-106) are set up. Each process line is labelled Set up 1 – Set up 3. Set up 1 and 2 have columns (T-101, T-102, T-103, and T-104) packed with untreated BC to test replicability of experiment. Set up 3's columns (T-105, T-106) are packed with acetic acid (4 M) treated BC to compare this treatment's effect on adsorption capacity. TK-101 is manually kept as consistently full of feed water as possible. TK-102, TK-103, and TK-104 are used to measure flowrates and volume of water treated by collecting outlet water. V-106, V-112, and V-118 are manual flow control valves. Flow is controlled at 1.05 L/hr. V-103, V-109, V-115 are manual valves used to sample column 1 outlet water.

b. Experiment 4.2.2

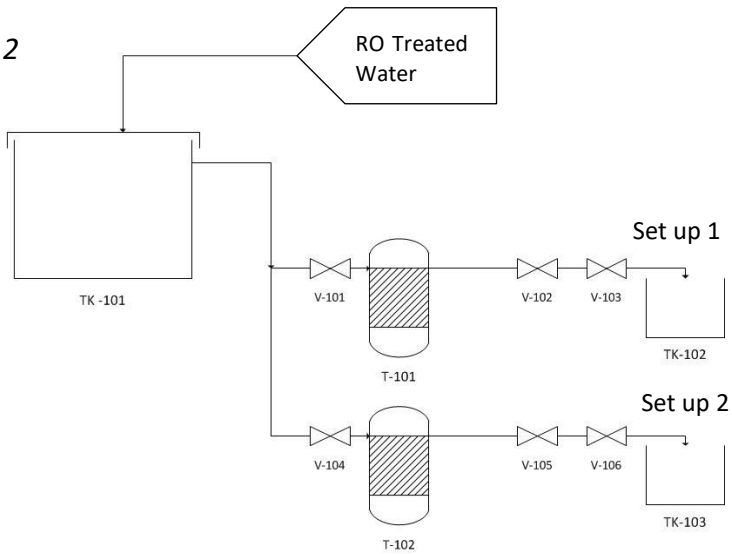

Figure 16: Experiment 4.2.2 schematic diagram

The saturated lead columns from experiment 4.2.1's set up 1 and set up 3 (T-101 and T-105 in Figure 15) are used *in* this experiment and positioned in the system as showed by Figure 16. A pipe connected to a reverse osmosis system connected to the feed tank provided reverse osmosis treated water as the carrier fluid for regeneration. Constant flowrate control was attempted (by manually adapting V-103 and V-106) at the start of the experiment; when the regeneration was observed to be very slow, however, flowrates were increased and not controlled as rigorously. Note that set up 2 was turned off before set up 1 due to dropping flowrates, and water conservation concerns.

c. Experiment 4.2.3

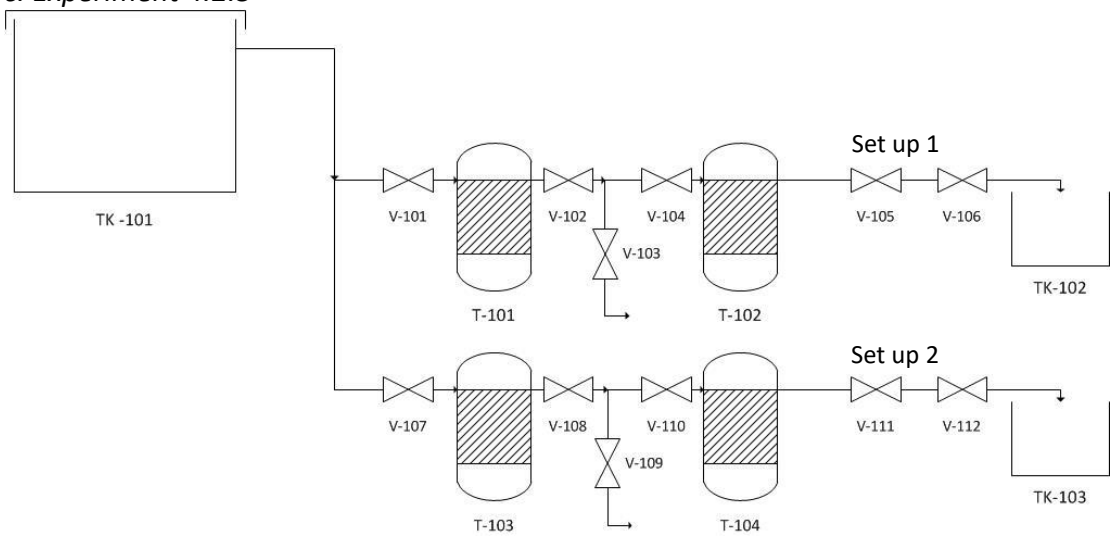

Figure 17: Schematic Diagram Experiment 4.2.3

Two process lines consisting two fixed beds in series (T-101 – T-104) are set up. Set up 1 is the process line with columns TK-101, and TK-102, while set up 2 consists of columns TK-103, and TK-104. All columns are packed with untreated BC; TK-101 is manually kept full of feed water. TK-102, and TK-103 are used to measure flowrates and volume of water treated. V-106, and V-112 are manual flow control valves. V-103, and V-109 are manual valves used to sample lead columns outlet water. Flowrates objectives for the two process lines are summarised in Table 7.

Table 7: Operating conditions experiment 4.2.3

Set up	Flowrate [L/hr]	Empty Bed Contact Time [hr]
1	2.1	0.33
2	1.6	0.44

4. Results and Analysis

Section 5 will present all experimental results, any background information for specific experiments not already covered, and brief analysis for individual experiments; it is

divided in two sub-sections, between kinetic batch experiments and fixed bed experiments, which are then further subdivided for each individual experiment. The errors included in the results only include apparatus errors.

4.1 Kinetic Batch Experiments

In sections 4.1.1 to 4.1.3, Equation 16 is used for all adsorption capacity calculations.

4.1.1 BC Charring - Varying Duration Comparison

a. Introduction

Due to information received from a similar collaborative organisation involved in BC production as a fluoride adsorbent, a possible improvement on standard BC production through further charring was investigated.

Hypothesis: *Charring BC by maintaining bones between 400-600°C for a further 2 – 4 hours to standard 1.5 hours, increases the final char's aqueous fluoride adsorption capacity.*

Type Experiment: 24 hour kinetic test
Average of doubles used for adsorption capacity calculation.
Adsorbent mass: 0.200g, 0.500g, 1.000g, 1.500g (± 0.0005g)
Volume of Water per test tube: 0.09 L (± 0.00005L)

Table 8: Experiment 4.1.1 feed water information

Feed Water Type	Fluoride Concentration	TDS	pH
Diluted Well Water	8.39 mg/L ± 0.3 mg/L	285	8.2

b. Results

Table 9: Experiment 4.1.1 calculated adsorption capacities – average of doubles

Burn Time [hr ± standard time]	*1.5 hr [standard]*	*1 hr [- 0.5 hr]*	*2.5 hr [+1 hr]*	*4 hr [+2.5 hr]*	*5.5 hr [+4 hr]*
Adsorbent Quantity [g]	Adsorption Capacity [mg/g]				
0.2	2.0 ± 0.1	1.3 ± 0.1	1.8 ± 0.1	1.8 ± 0.1	2.0 ± 0.1
0.5	1.23 ± 0.02	1.23 ± 0.02	1.25 ± 0.02	1.20 ± 0.02	1.24 ± 0.02
1	0.687 ± 0.009	0.674 ± 0.009	0.692 ± 0.009	0.684 ± 0.009	0.684 ± 0.009
1.5	0.463 ± 0.006	0.447 ± 0.006	0.463 ± 0.006	0.462 ± 0.006	0.458 ± 0.006

Table 10: Inclusive range of adsorption capacities for different burn times

Adsorbent Quantity [g]	Range of Adsorption Capacities [mg/g]
0.2	1.70 ± 21 %
0.5	1.22 ± 2.5 %
1	0.683 ± 1.3 %
1.5	0.455 ± 1.8 %

c. Analysis

For all the adsorbent quantities tested, except for 0.2g, insignificant variation in adsorption capacity for BC charred for different time durations is calculated. The greatest variation in adsorption capacities amongst these quantities is only 2.5%. A greater variation is present for the adsorption capacities calculated for the smallest adsorbent mass (0.2g of BC); the variation between adsorption capacities for this quantity is 21%. The fluoride concentration measurement error explains all variations, as well as this anomaly. The greatest relative error of the adsorption capacity values calculated for 0.2 g of adsorbent is 11.3 %. For all other adsorbent masses' adsorption capacities calculated, the relative error is below 2 %. The variation outside of the stated apparatus error is attributed to human error in measurements, and time of removal of adsorbent.

The adsorption capacity error increases as the adsorbent mass decreases. Adsorption capacity absolute error includes the addition of the feed water fluoride concentration (c_0) error and the outlet water fluoride concentration (c_t) error, refer to Equation 15 for the adsorption capacity equation. For a smaller adsorbent mass, in the same volume of contaminated water, less fluoride will be adsorbed and the final concentration (c_t), therefore, will be greater than that of samples with greater adsorbent mass. The fluoride concentration colorimeter, as explained in Section 3.2.1, requires dilution for samples with fluoride concentrations greater than 2 mg/L; the dilution factor also multiplies the standard error of 0.06 ± mg/L to give the final concentration value's error. The smaller the adsorbent mass is in the concentrated sample, therefore, the greater the fluoride concentration measured will be when testing the sample after time t; thus resulting in the greater overall adsorption capacity error.

This experiment discredited the hypothesis that further charring the BC would improve aqueous fluoride adsorption capacity for local well groundwater.

4.1.2 Commercial Arsenic Adsorbents Comparison

a. Introduction

Hypothesis: *One of the selected affordable commercial aqueous arsenic adsorbents (Bayoxide ® E33, Bayoxide ® E33 HC, and TiO_2 with sand particles) has a superior adsorption capacity for the local groundwater chemistry.*

Type Experiment: 24 hour kinetic test

Average of doubles used for adsorption capacity calculation.
Adsorbent mass: 0.005g, 0.010g, 0.050g, 0.100 g (± 0.0005g)
Volume of Water per test tube: 0.09 L (± 0.00005L)

Table 11: Experiment 4.1.2 feed water information

Feed Water Type	Arsenic Concentration	TDS	pH
Diluted Well Water	40 µg/L ± 5 µg/L	285	8.2

b. Results

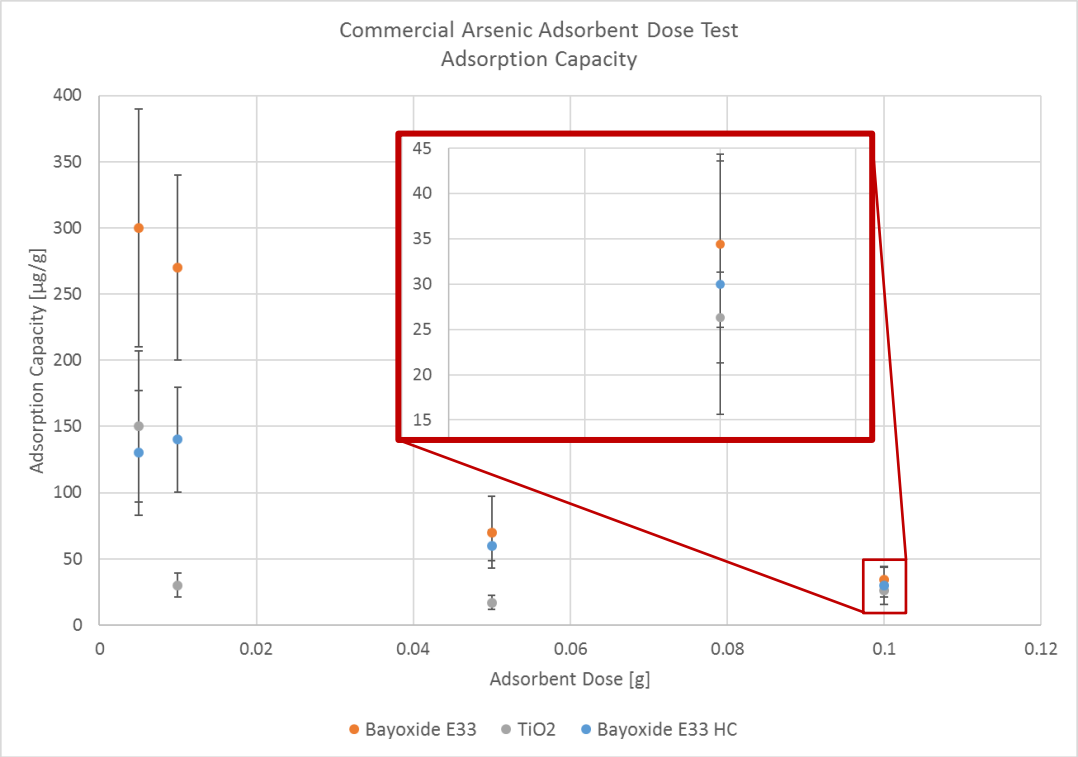

Figure 18: Experiment 4.1.2 average adsorption capacities

Table 12: Summary of calculated parameters experiment 4.1.3

\\Adsorbent Name Mass Adsorbent [g]\\	Average Adsorption Capacity [µg/g]		
	Bayoxide ® E33	TiO_2	Bayoxide ® E33 HC
0.005	300 ± 90	150 ± 60	130 ± 50
0.01	280 ± 70	30 ± 9	150 ± 40
0.05	70 ± 30	17 ± 5	60 ± 10
0.1	34 ± 9	26 ± 5	30 ± 10

c. Analysis

Unfortunately, as illustrated by Table 12, even if Bayoxide ® E33 consistently tested with the highest adsorption capacity calculated – the error on the results for 0.05 g and 0.1 g

of adsorbent are too large to conclude Bayoxide ® E33 has the highest adsorption capacity for those doses.

Similarly to the fluoride concentration test, the arsenic field test kit used inherently has a larger absolute error for higher arsenic concentrations, see section 3.2.1 for a full error list. The nature of the arsenic field test kit used also includes more human error than the fluoride test; arsenic field test errors are discussed further in section 5.1.2 and in Appendix D. For adsorbent doses 0.005g, and 0.01g, however, regardless of the large error, Bayoxide ® E33 tested conclusively with the highest adsorption capacity. The doubt resulting from these results' errors, lead to the decision of testing TiO_2 (which was calculated to have the lowest adsorption capacity in this experiment but has a distinct chemical structure compared to the two Bayoxide variations) alongside Bayoxide ® E33 in the 1-week long batch kinetic model experiment, experiment 4.1.3.

Results suggested that Bayoxide® E33 has the highest adsorption capacity for aqueous arsenic for the local groundwater chemistry out of adsorbents tested; errors in measurements, however, impede a definite conclusion.

4.1.3 Commercial Arsenic Adsorbents Kinetic Test
a. Introduction
Hypothesis: *Both adsorbents will rise to saturation adsorption capacity in first few hours of experiment and when saturation is reached adsorption capacity will remain constant for rest of experiment. Bayoxide ® E33 is expected to reach higher saturation capacity than TiO_2.*

Type Experiment: 1 week batch test
Average of doubles used for adsorption capacity calculations.
Adsorbent mass:
Bayoxide ® E33: 0.005g ± 0.0005g; TiO_2: 0.080 ± 0.0005g
Volume of Water per test tube: 0.09 L (± 0.00005L)

Table 13: Experiment 4.1.3 feed water information

Feed Water Type	Arsenic Concentration	TDS	pH
Diluted Well Water	40 µg/L ± 5 µg/L	285	8.2

b. Results

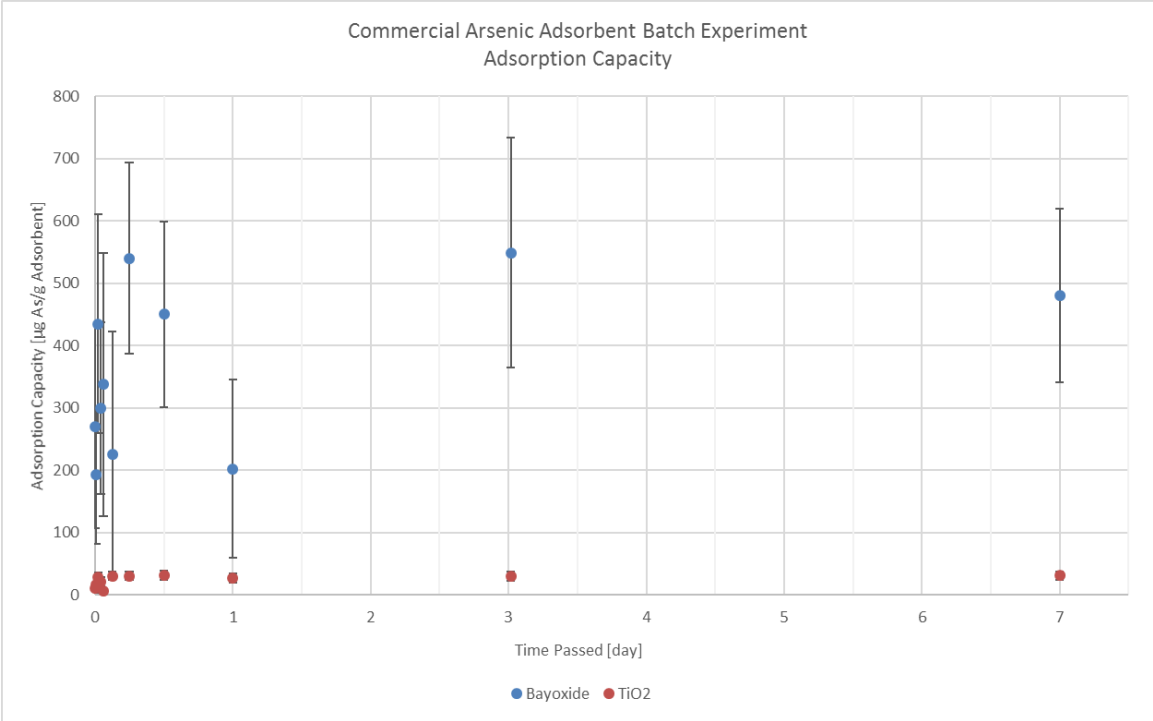

Figure 19: Bayoxide ® E33 and TiO2 adsorption capacity over 1 week batch experiment

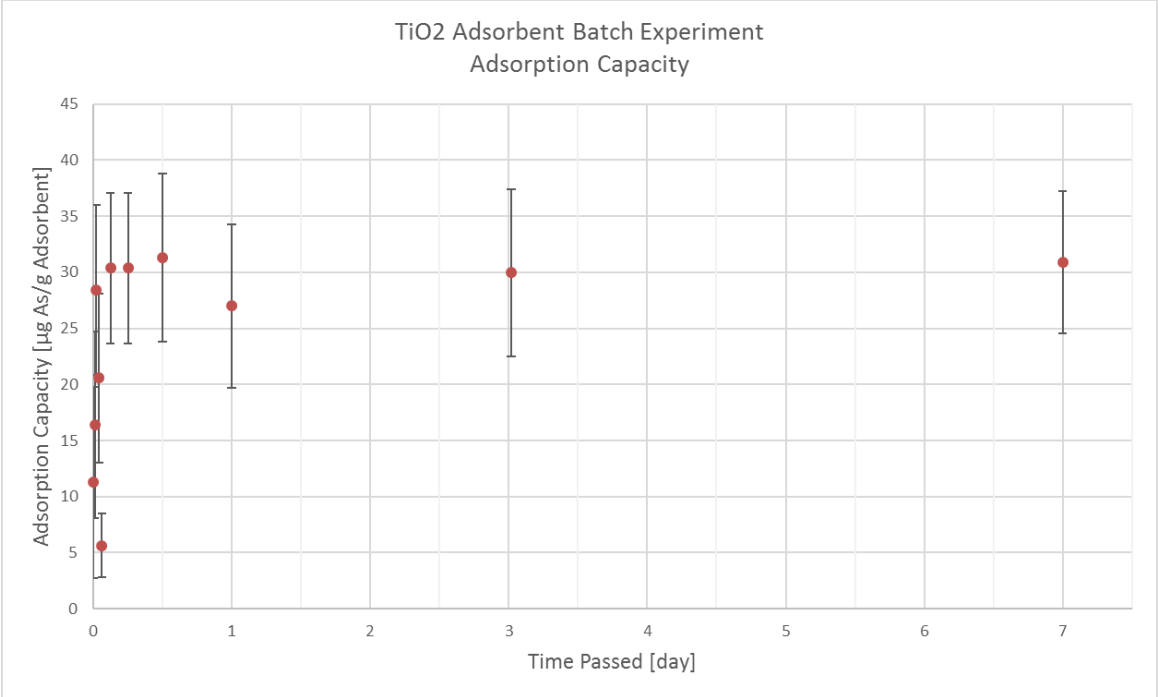

Figure 20: TiO2 adsorption capacity over 1 week batch experiment

Table 14: Saturation adsorption capacity

	Time taken to reach *[days]*	**Average saturation adsorption capacity** *[µg As/g Adsorbent]*	**Variation in saturation adsorption capacities** *[%]*
Bayoxide ® E33	0.25	500 ± 100	± 10
TiO_2	0.13	30 ± 7	± 7

c. Analysis

The results from this experiment exhibit presence of experimental noise and significant variation between the doubles tested; variation between doubles was in certain cases higher than the arsenic test errors. This higher error than expected could be attributed to competing species interference with the arsenic test kits, human error, or a combination of these factors. Note that the adsorption capacity calculated for Bayoxide ® E33 after one day of the experiment is very low and considered an unreliable anomalous value.

All calculated adsorption capacities are plotted and shown in Figure 19 and Figure 20; the error is noticeable in the graphs, with certain tested samples for Bayoxide ® E33 exhibiting significantly lower adsorption capacity than expected (noticeably, the samples tested after 0.13, 0.5 and 1 day). It is still possible to observe, however, adsorption capacity increasing in the first few hours of the experiment and approaching a saturation value for both adsorbents. An average of the saturation adsorption capacities was taken (excluding the significantly lower experimental anomalous value calculated after 1 day) and summarised in Table 14 alongside the time taken to have been reached. TiO_2 exhibits faster kinetics than Bayoxide ® E33, reaching adsorption capacity in slightly over half the time taken by Bayoxide ® E33. Regardless of the significant error noticed, the Bayoxide ® E33 saturation capacity is an order of magnitude greater than TiO_2; thus confirming its superiority as an aqueous arsenic adsorbent in the feed water chemistry used. A second validating experiment should be run in the future to validate the results due to the variation between doubles observed in these results.

4.2 Fixed Bed Experiments

For section 4.2, Equation 18 is used for all adsorption capacity calculations using the trapezoidal rule to integrate Excel data. Table 15 provides feed water information for all experiments discussed in section 5.2. The pressure drop estimations presented in Table 20, were calculated using the parameters listed in section 4.5.2 and Equation 12 - Equation 14.

Table 15: Feed water information experiments 4.2.1 – 4.2.3

Feed Water Type	Fluoride Concentration	TDS	pH
Diluted Well Water	8.5 mg/L ± 0.3 mg/L	285	8.2

4.2.1 Acid Treated and Untreated BC Fluoride Adsorption: Fixed Bed

a. Introduction

Hypothesis: A*cid treated BC will perform better than untreated BC; overall filter system will take at least 21 days to breakthrough with a constant flowrate. Family-size filter system modelling.*

Type Experiment: Continuous Flow Fixed-bed

b. Results

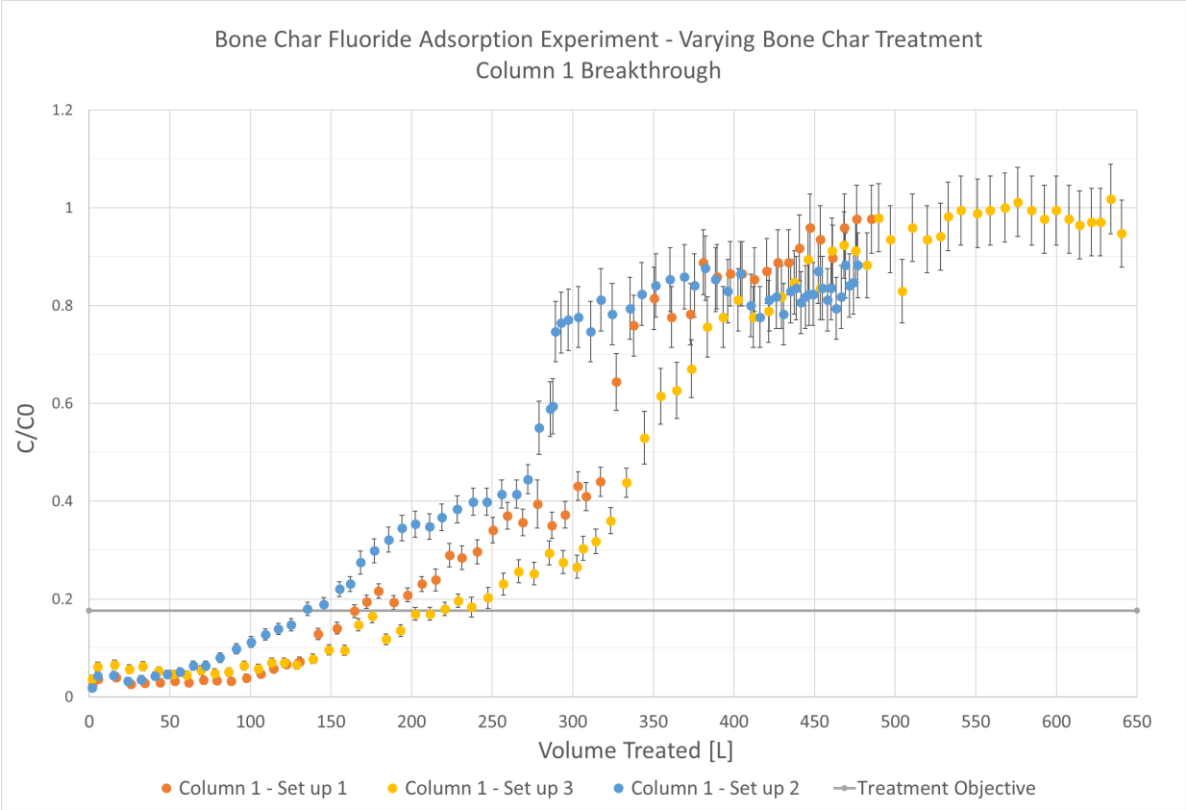

Figure 21: Experiment 4.2.1 column 1 breakthrough curves

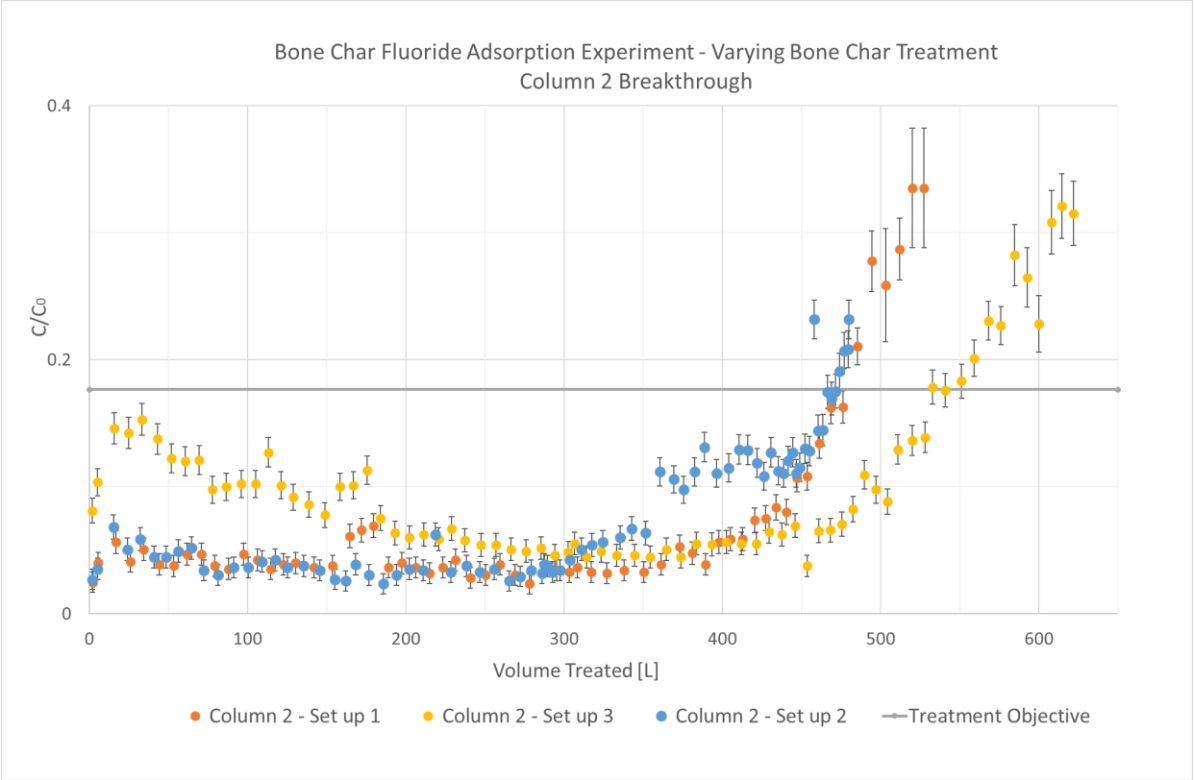

Figure 22: Experiment 4.2.1 column 2 breakthrough curves

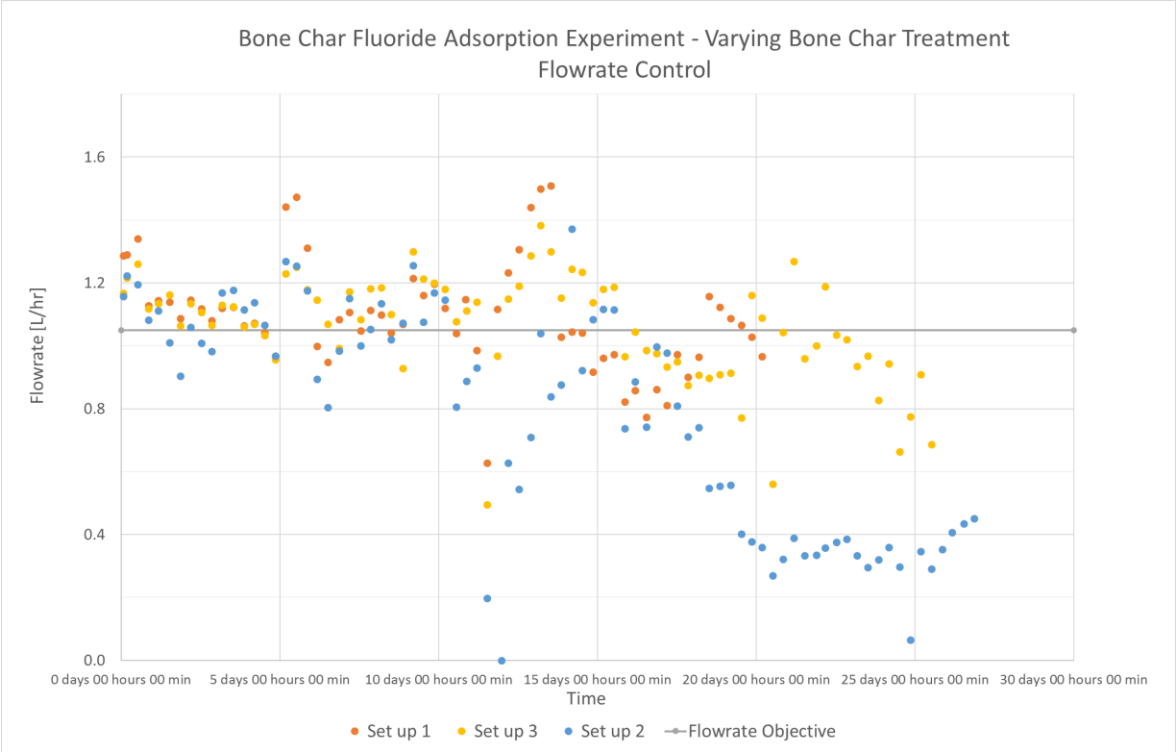

Figure 23: Experiment 4.2.1 flowrate control

Table 16: Summary of calculated parameters – experiment 4.2.1

	Set up 1	Set up 2	Set up 3
Adsorption Capacity *[mg/g]*	5.8 ± 0.4	5.2 ± 0.3	6.2 ± 0.4
Breakthrough time of Treatment Objective (Full System)	18 days and 4 hours	25 days and 12 hours	22 days and 12 hours
Volume Water Treated before breakthrough of Treatment Objective (Full System) *[L]*	476 ± 2	474 ± 2	551 ± 2

c. Analysis

i. Dropping Flowrates

As shown by Figure 23, the manual flowrate control method used to maintain a constant flowrate, which is also dependent on the water level in the feed tank, resulted in a significant fluctuation of flowrates throughout the experiment. Although the manual control throughout the whole experiment caused flowrate disturbances, a significant decrease in flowrates began after 17 days for set up 2, and after 21 days for set up 3. The manual valve control, even when left completely open, resulted in significantly slower flowrates. A more comprehensive analysis of this process problem is provided in section 5.1.1 of the critical analysis.

ii. Set up 1 and Set up 2 Comparison

Set up 1 and set up 2 are identical systems, both packed with untreated BC adsorbent. These set ups serve the purpose of testing the replicability of results; the calculated adsorption capacity and breakthrough time for each set up are summarised in Table 16. Unfortunately, due to set up 2's dropping flowrates the systems experienced varied operation conditions. This explained the 29 % greater breakthrough time exhibited by set up 2. The calculated adsorption capacities have a 10% difference, and the water treated volumes a 0.4 % difference; experimental error in measurements and operation condition variations account for these smaller variations. The systems, however, exhibited replicability of results and confirmed the calculated adsorption capacity.

iii. Untreated and Acid-Treated BC Comparison

Set up 3's purpose was to compare acid treated BC to untreated BC (acid treatment methodology is outline in Appendix A.1.3). The acetic acid treated BC performed better than the untreated BC, as expected. Compared to set up 1, the acid treated char has a 6% higher adsorption capacity and 13% larger volume of water treated before the treatment objective breakthrough. Compared to set up 2, a 16% higher adsorption capacity and 14% larger volume of water treated before breakthrough were calculated. This improvement is accounted to by the possibility of surface area increase due to acid treatment, as well as a decrease in pH of the BC surface which, as explained in section 3.3.1, increases BC's affinity for fluoride ions. In Figure 22, an initial increase in concentration is observed in set up 3 at roughly 10 L of water treated, this increase is not a real reflection but is caused by a phosphate ion interferences with the fluoride

testing. This interference is addressed in experiment 4.2.3 by flushing the BC with RO treated water before commencement of the experiment (as mentioned in Section 3.3).

4.2.2 Desorption Experiment Acid Treated and Untreated BC: Packed Bed
a. Introduction
Hypothesis: *Reverse Osmosis treated water is a successful carrier solution to regenerate fluoride saturated BC. Desorption is expected to be a slower process than adsorption, furthermore acid treated BC will take a longer period of time to regenerate completely compared to untreated BC.*

Type Experiment: Continuous Flow Fixed-bed
b. Results

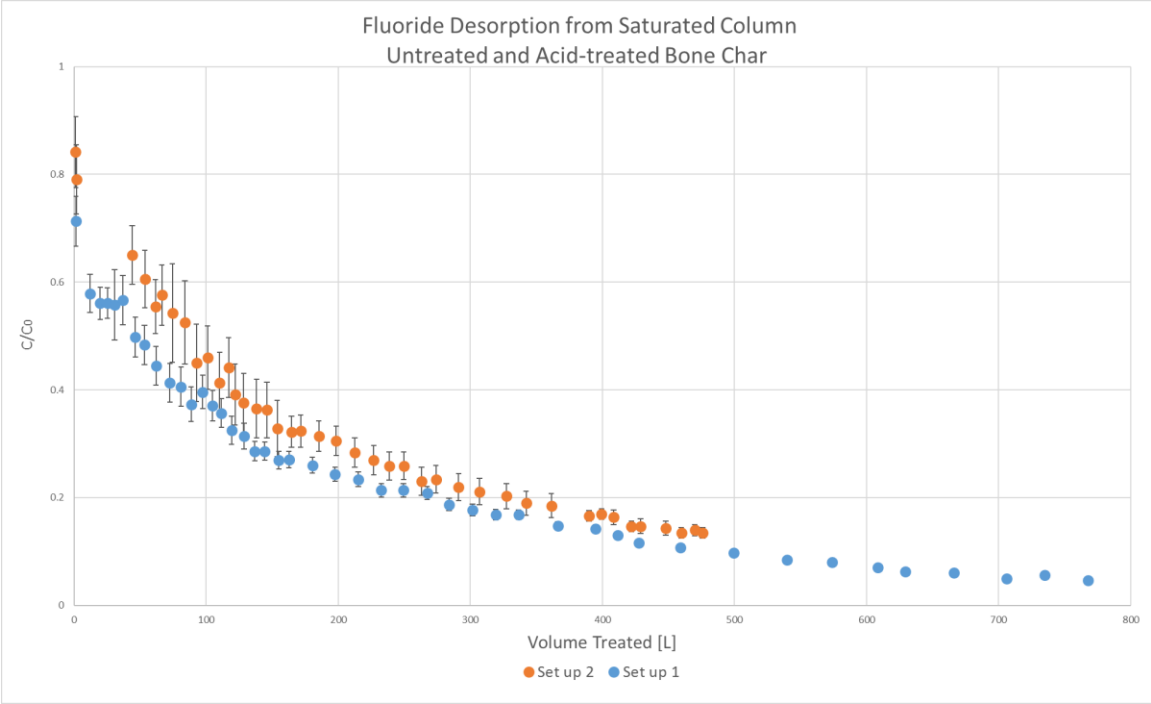

Figure 24: Outlet fluoride concentration – desorption experiment 4.2.2

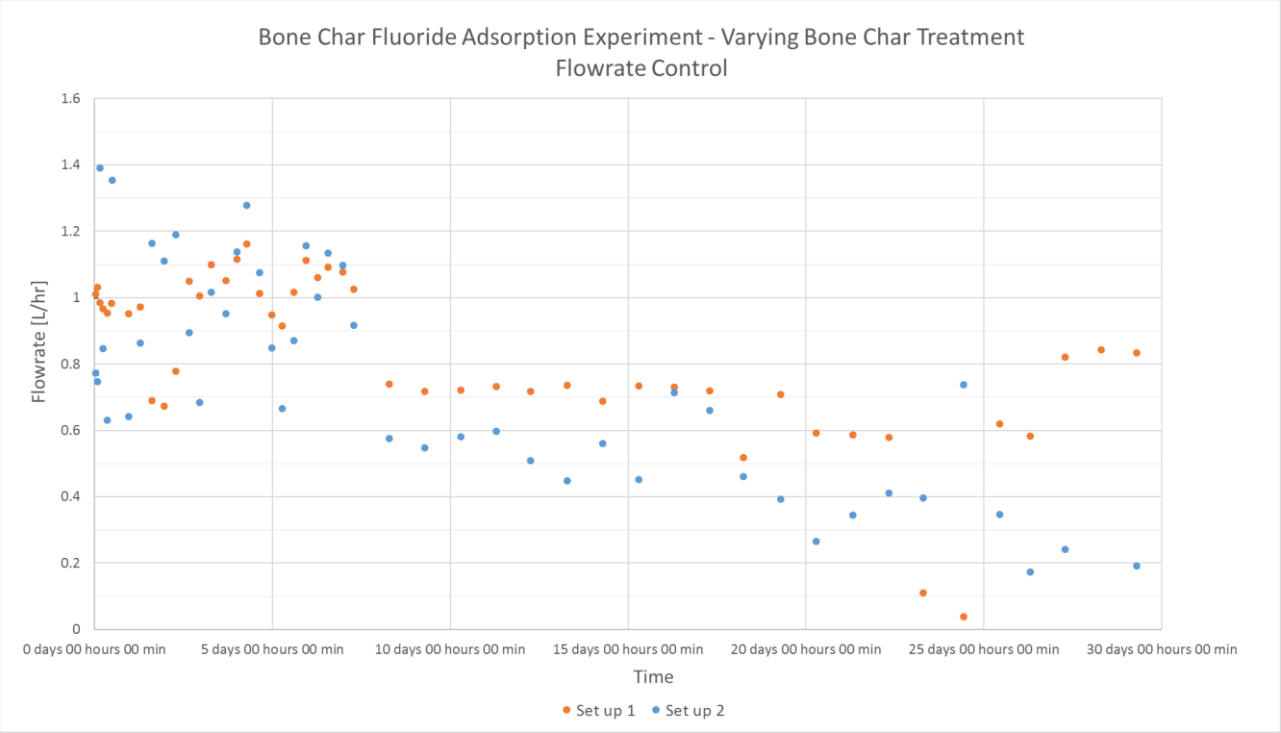

Figure 25: Experiment 4.2.2 flowrate monitoring

Table 17: Summary of calculated parameters – Experiment 4.2.2

	Set up 1	Set up 2
Amount Fluoride Desorbed throughout Experiment *[g]*	1.2 ± 0.1	1.2 ± 0.1
Percent of Saturated Column Desorbed *[%]*	50	47
Volume of Carrier Passed through system *[L]*	767 ± 2	476 ± 2

c. Analysis

i. Set up 1 and Set up 2 Comparison

Set up 2, compromised of the bed packed with acid treated BC, desorbed more fluoride than set up 1, with bed packed with untreated BC. When comparing the amount of fluoride desorbed after 476 L of carrier were passed through the system (the time set up 2 was turned off), set up 1 desorbed 1.0 g while set up 2 desorbed 1.2 g of fluoride; there was therefore a 20% increase in desorbed fluoride in the acid treated BC. Since the acid treated BC had a higher adsorption capacity than the untreated one, this can be explained by a larger amount of fluoride being in the saturated set up 2 system.

iii. Speed and Shape of Desorption Profile

As expected, desorption slowed down as more carrier desorbed fluoride from the saturated char due to a decrease in driving force (which is the chemical potential but

can be closely estimated with the concentration difference) of the process. After 767 L of carrier had passed through the set up 1 column, only 50 % of adsorbed fluoride was removed from char. Reverse osmosis treated water is not an effective carrier for regeneration due to its lack of effectiveness and its energy intensive necessary treatment. Future experiments with salt water, or acid or base treated water, as a carrier can be run to investigate other possible regeneration practices.

4.2.3 Adsorption Experiment Varying Flowrates: Packed Bed

a. Introduction

Hypothesis: *Investigation of replicability of results for BC fixed bed is tested through increasing flowrates.*

Type Experiment: Continuous Flow Fixed-bed

b. Results

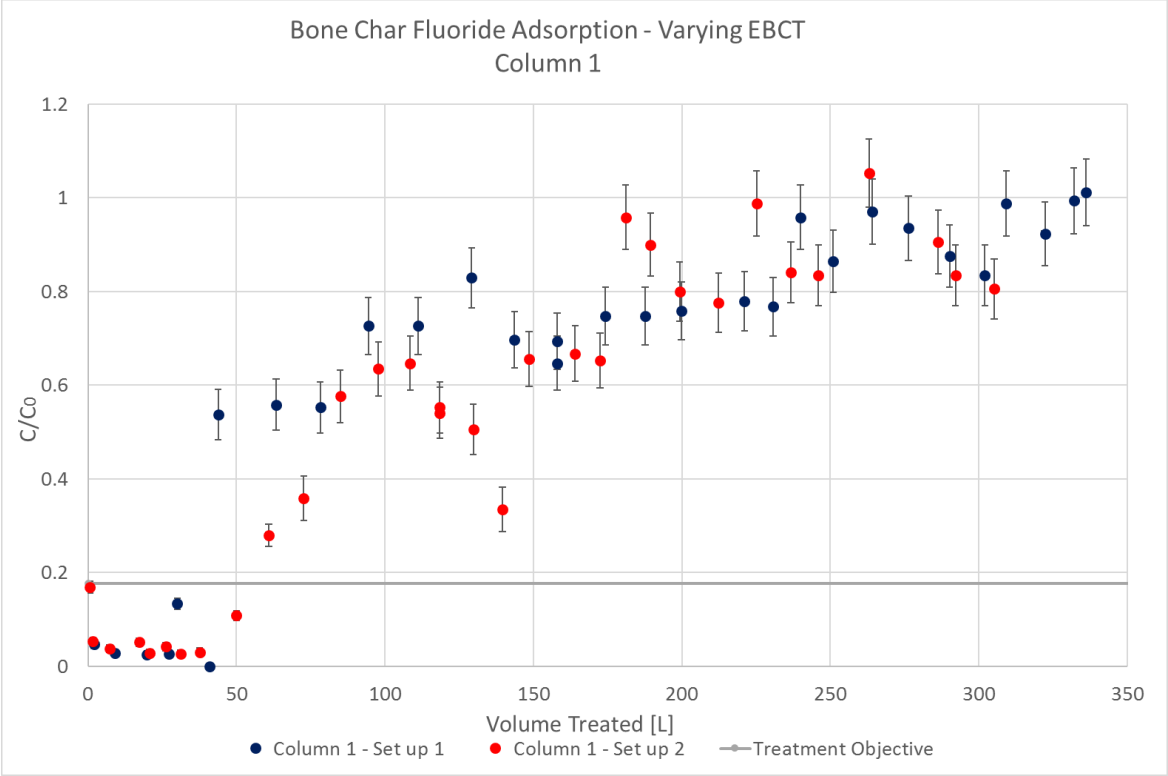

Figure 26: Experiment 4.2.3 column 1 breakthroughs

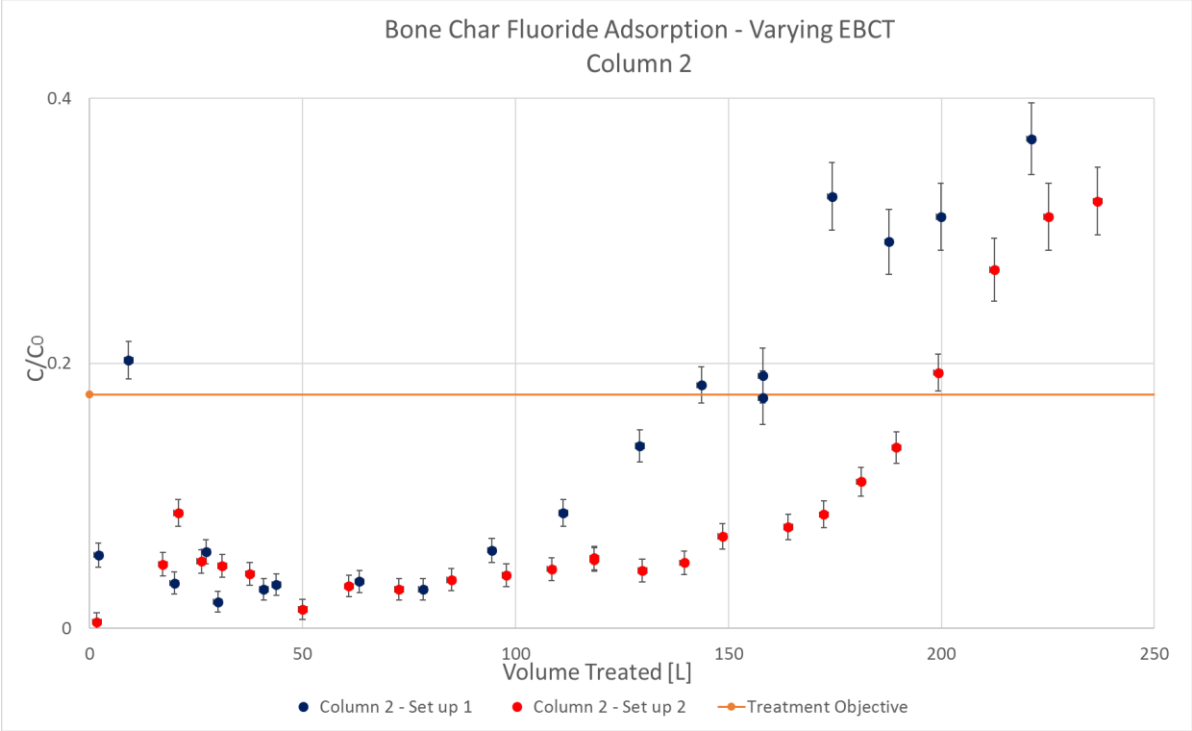

Figure 27: Experiment 4.2.3 column 2 breakthroughs

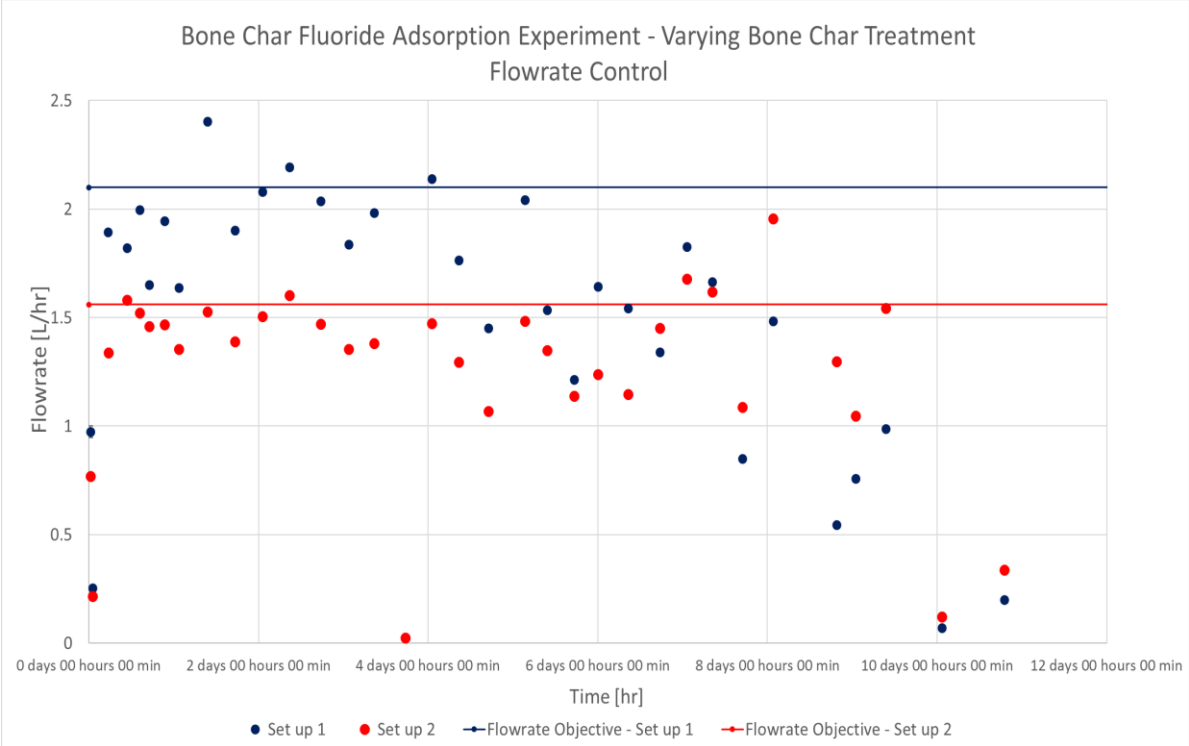

Figure 28: Experiment 4.2.3 flowrate control data

Table 18: Summary of calculated parameters experiment 4.2.3

	Set up 1	Set up 2
Adsorption Capacity per column *[mg/g]*	3.2 ± 0.2	3.1 ± 0.2
Breakthrough time of Treatment Objective (Full System)	5 days and 13 hours	7 days and 21 hours
Volume Water Treated before breakthrough of Treatment Objective (Full System) *[L]*	188 ± 2	211 ± 2

Table 19: Summary of EBCT variation

Empty Bed Contact Time *[hr]*	0.66	0.44	0.33
Volume Water Treated before breakthrough of Treatment Objective (Full System) *[L]*	475 ± 2	211 ± 2	188 ± 2
Adsorption Capacity per column *[mg/g]*	5.5 ± 0.3	3.1 ± 0.2	3.2 ± 0.2

Table 20: Friction factors estimation

Empty Bed Contact Time *[hr]*	0.66	0.44	0.33
Pressure Drop over column *[Pa/m]*	22.0	33.5	44.0

c. Analysis

i. Column 1 Breakthrough Results Reliability

Figure 26 graphically illustrates the column 1 breakthrough curves of both set ups. The small variation of 3 % in adsorption capacity between the two set ups indicates equilibrium controlled adsorption is taking place. The difference between these set ups and set ups 1 and 2 of experiment 4.2.1 can be explained by variation in column packing, refer to Section 5.1.3 for further discussion of this variation, or by the BC flushing pre-treatment completed for this experiment. Note that the friction factors presented in Table 20 are only estimations due to the estimated value of bed void fraction based on literature values of BC which vary extensively in literature. An experiment aimed at calculating BC density is recommended to be conducted in the future to allow more accurate bed void fraction calculations.

The results include significant experimental noise and, although they show a general breakthrough pattern, the inconsistency and fluctuations of the results undermine the results' reliability. The possible reasons explaining the poorer quality of results compared to Experiment 4.2.1's include: human error, variation in feed water fluoride concentration, frequency of samples taken, and flowrate inconsistency.

The apparatus error is included in the graphs and for all calculated values. The experimental procedure for the fixed bed experiments give room for substantial human error. Two technology team members were responsible for this experiment's samples collection and testing; therefore, a greater negative effect on results' accuracy may have arisen due to human error for this experiment. Moreover, the feed water for all fixed bed experiments, as explained by section 3.4.1 and Appendix B, is mixed and diluted and

tested to ensure constant concentration of 8.5 ± 0.2 mg/L; this procedure is performed per 1m^3 of water. The feed water is further tested at each sampling time to monitor the consistency of concentration. For this experiment it was noted as the feed water was tested during the experiment had a greater variation in concentration (7.9 mg/L – 9.7 mg/L). Although methodology was followed, failure in perfect mixing or misleading testing checks before the experiment commencement negatively impacted feed water concentration consistency. Furthermore, compared to experiment 4.2.1's sampling frequency, this experiment due to the higher flowrates was sampled less frequently in relation to volume of water treated. This results in less data points, and therefore any variation and error of samples tested affects the general concentration trend and overall accuracy of the breakthrough curve more significantly. Lastly, the flowrate drops noted in all fixed bed experiments were more drastic and dramatic for this experiment. The higher flowrates attempted result in higher pressure drop throughout the fixed bed and therefore greater flowrate drops are observed and affect the consistency of the system.

ii. Column 2 Results – Variation of Empty Bed Contact Time

The column 2 breakthrough curve results (illustrated graphically in Figure 27 are significantly more consistent and result in the expected quicker breakthrough time of set up 1 compared to set up 2. A comparison of this experiment's results to the averaged results of experiment 4.2.1's untreated BC breakthrough of treatment objective is summarised in Table 19. The near overlap of the breakthrough curves when plotted against volume of solute passed through system suggests an equilibrium limited adsorption process. The flowrate control failures affected the EBCT consistency significantly. Despite of this control failure, the general trend of EBCT proportionality to breakthrough time is sustained by experimental results.

4.3 Mass Balance

Equation 15, for batch experiments, and Equation 22 for column experiments, describe the mass balance calculations conducted for the experiments. The mass balances do not take into account dispersion effects or heat transfer contributions. The measured amount of contaminant introduced to each experimental system, the sum of accumulated amount and measured outlet amount, and the percentage disparity between the two values are presented in Table 21 for experiments 4.1.1 to 4.1.3.

$$\int_{t_0}^{t} c_0 Q_t = \int_{t_0}^{t} c_t Q_t + q_t m_s \qquad \textit{Equation 22}$$

For experiments 4.1.1 – 4.1.3, the values presented are sums of all samples tested, including all doubles, and therefore include relevant variations. Column experiments', 4.2.1 -4.2.3, mass balance calculations are not presented because the accumulation term, $q_t m_s$, contains the adsorbed amount value which was calculated with Equation 18; Equation 18 is just a rearrangement of Equation 22, therefore the mass balance comes out to balance perfectly for each experiment with 0 % disparity. A more rigorous mass balance using Equation 17 should be conducted for future experiments; due to the

experimental objective scope of this report, the large apparatus error, the significant uncertainty of the empty bed void fraction value (calculated based on literature BC density values that vary significantly in literature), and time constraints, the more rigorous calculation was not conducted for experiments 4.2.1 – 4.2.3.

Table 21: Mass balances for experiments 4.1.1 – 4.1.3

Experiment	F or As	In *F [mg], As [μg]*	Accumulated + Out *F [mg], As [μg]*	Disparity *[%]*
4.1.1	F	1300 ± 100	1500 ± 100	13 %
4.1.2	As	3020 ± 300	3210 ± 300	6 %
4.1.3	As	7100 ± 800	9100 ± 900	22 %

The mass balance percentage disparities of experiments 4.1.1 and 4.1.2 are explained by the error of the testing and measuring apparatus. Experiment 4.1.3 exhibited larger errors and variations between doubles, this is reflected in the larger percentage disparity presented; a discussion on experiment 4.13's error is available in section 4.1.3.

5. Critical Analysis

Following the experiments-specific analysis offered for each experiment within section 4, section 6 will critically analyse the issues affecting numerous or all experimental results, as well as offer a reflection on potential future improvements.

5.1 Issues Encountered and Proposed Solutions

5.1.1 Flowrate Control

The most problematic experimental issue encountered across experiments was the dropping flowrates observed in all column experiments, especially in experiment 4.2.3. From Figure 23, Figure 25, and Figure 28, it is noticeable that flowrates decreased dramatically over time, and that the decrease speed increased for fixed bed systems at higher flowrates. This is explained by the higher pressure drops experienced by systems with higher flowrates, in otherwise identical systems. All flowrates tested throughout the experiments are in the laminar flow regime, with Reynolds numbers estimated at 3.5, 5.4, and 7.1 for column flowrates 1.05 L/hr, 1.6 L/hr, and 2.1 L/hr respectively. In this regime, in fact, pressure drops are proportional to superstitial fluid velocity, and inversely proportional to bed void fraction (assuming constant fluid density and viscosity) (Perry & Green, 2008). Three possible explanations and contributions to the dropping flowrates, involving bed void fraction, fouling, and the manual control system, are discussed below.

Due to the incompressible nature of water, running the columns over an extended period of time may cause movement in the granular media within the bed; thus creating non-homogenous bed void fraction areas. This would increase pressure drops and result in flowrate reduction. Furthermore, the feed water used originates straight from a well and is stored in a sealed storage unit outdoors for long periods of time. It is possible,

therefore, solid particles or impurities are introduced in the feed water; mechanical obstruction from these particles may in turn result in fouling within the system. Moreover, the flow control system of the columns is currently completely manual and dependent on the feed storage tank water level, which consequently introduces errors and variations in addition to the flow fouling problems.

A number of experiments can be conducted to determine the dominating flow hindering factor and general improvements to the system can improve the flow control reliability. Increasing and stabilising the bed void fraction within the fixed bed by introducing a different material may mitigate this issue; metal mesh perpendicular to flows at different cross sections of the fixed bed or sand particles may suspend the granular adsorbent media more successfully, and increasing adsorbent particle size, or introducing thin steel rods or vessels can mitigate the flowrate issues related to pressure drop and homogeneous bed void fraction. Although these modification would decrease the amount of adsorbent within the column, and therefore decrease adsorption capacity, for a scaled up design which takes into account these reductions in adsorption capacity the treatment objectives can still be met while ensuring consistent flow.. Furthermore, introducing a filter, upstream of the first column but downstream of the feed tank, will remove particles that may cause interferences. Additionally, introducing a second upstream feed storage tank and a float level valve on the feed storage tank immediately upstream of the fixed beds, can remove the flowrate dependence of head level variation. Lastly, ensuring that the system is run at the slowest possible flowrate, will assist in maintaining low pressure drops and constant flowrates.

5.1.2 Arsenic Test Kit Error and Experimental Noise

The arsenic field test kits used to test water samples, tested with significant error. To decipher the test concentration result, the colour on a test strip needs to be matched to a colour palette provided by the kit. This procedure can introduce significant human error and variation depending on who is performing the test as well as introduces other visual variables. In addition to the test kit's intrinsic error, the kits provided unexpected test results multiple times when testing water of known arsenic concentration. During the placement, roughly two months were spent attempting to mitigate this worrying phenomenon and to quantify the observed errors. Through a number of tests of both groundwater samples and prepared arsenic standard solutions, as well as a statistical analysis, a report concluding the ITS ® Quick arsenic field tests were acceptably reliable for experimental aims was produced (see Appendix D). The extremely low concentrations of aqueous arsenic that need to be measured to ensure potable water quality, as well as financial limitations of the Caminos de Agua laboratory setting, result in a limited possible mitigation methods to this experimental analysis hindrance (Smedley & Kinniburgh, 2013)After these testing difficulties arose, the decision to periodically send tested samples to an accredited laboratory to validate results was made; this will add more certainty and security to future experimental results.

5.1.3 Variance in Experiments

Although valuable comparison data was achieved with experimental results, variation in BC treatment (discussed in Section 3.3) and in BC packing present between experiments 4.2.1 and 4.2.3, introduces uncertainty undermining the conclusions drawn between the two experiments. The amorphous nature of BC, as well as its production method, inherently introduce uncertainty for parameters including pore size distribution, average particle size, adsorbent density and structural chemistry. Additionally, the feed water chemistry between experiments may also experience changes. For each individual experiment, a volume of 100 m^3 of feed water was prepared, mixed, and diluted prior to each experimental run; therefore the water chemistry was consistent for each experiment, as summarised in section 3.4.1. Between experiments, however, it is possible that the water chemistry varied due to natural variations in groundwater competing species and pH. These variations may affect the results of different experiments and should be noted especially for comparison between experiments 4.2.1 and 4.2.3 results, which present data which is valuable for comparison but with potential variations in BC pre-treatment and packing, and in feed water chemistry.

While the feed water variance is acceptable given the objective of the experiments of assessing adsorption capacity for the specific water in question, minimising variance in pre-treating, packing, and producing the adsorbent through careful measurement and quantitative methodologies can increase reliability of future experimental results. Weighing the amount of adsorbent within individual column sand the adsorbent densities as accurately as possible multiple times, is a crucial step for valuable conclusions drawn from comparison among different columns' experimental results.

5.2 Suggestions for future experiments

5.1.4 *Temperature and pH Dependence*

As mentioned in background section 3.3.1, literature experimental results indicate fluoride BC adsorption is independent of temperature between 15 – 35 °C (Medellin-Castillo & et.al., 2014). An ion exchange mechanism occurring between the fluoride ions and the BC surface, can explain this independence due to the relatively low, of usually below 9 kJ/mol, enthalpy changes (Helfferich, 1995). During experiment 4.2.3, however, the experimental set up was located outdoors and ran consequently for over 7 days; temperatures in San Miguel de Allende in December span from -2°C to 26°C reference, over the 24 hours. This is a greater temperature variation than the one tested for in literature and may affect the consistency of adsorption mechanisms in the final filter design. The variation's effect on adsorption capacity could be easily tested by comparing 24-hour kinetic test results in a fridge set to a temperature of 0°C to kinetic test results ran at the standard room temperature of roughly 15°C (with insulation maintaining the water at as constant a temperature as possible). Due to the lower adsorption capacity noted in the BC in experiment 4.2.3 compared to experiment 4.2.1, during which temperatures did not drop below 15°C throughout the experiment, the temperature dependence experiment is worth running.

The concept of point of zero charge was introduced in section 3.3.1; due to electrostatic forces between adsorbent and adsorbate the water pH position relative to the point of zero charge of a system significantly affects adsorption capacity, as explained in section 3.3. The literature review of aqueous fluoride and arsenic adsorption indicates a lower pH than the current average well water of pH 8.5, favours adsorption of both species. Although the pH effect on adsorption is well understood, the decision to avoid chemical treatment to feed water through acid and base addition was made to avoid introducing complexities that will be problematic to implement in the final filter. Investigating the extent of pH effect on adsorption performance is however a worthwhile experiment due to possible variations in well water pH. This investigation may be conducted with batch experiments with acid and base treated feed water and pH monitoring. The comparison between adsorption capacities with a range of pH feed waters allows calculation of pH effect on adsorption capacity.

5.1.5 *General next steps for filter goal*

As discussed at the termination of the placement, the next experimental priority entails testing continuous fixed bed with the Bayoxide ® E33 adsorbent to ensure its effectiveness and estimate the lifetime of arsenic column breakthrough. Once the effectiveness of both adsorbents is ensured, the final scaled up design will need to be finalised and tested. Due to its longer lifetime, a larger community-sized filter was concluded to be a better design than the smaller family-size filter (as per the size of fixed bed experiments presented in section 4). The design of this larger filter will continue to adopt the 'lead lag', two columns in series (as per the design set up introduced in section 1.3.3). Particular care and experimental focus should lie in ensuring axial dispersion and consistent flow, a particularly problematic parameter for liquid flows through beds with large diameters. Further investigative experiments can include varying feed concentrations to investigate the effect of varying chemical potential differences on adsorption performance and to investigate the adsorption isotherm that can most closely fit the filter system.

6. Conclusion

6.1 Project and Results Summary

The research presented in this report was completed over a course of six months within Caminos de Agua's Technology and Development team. The research contributes to the development of an adsorption filter aimed at removing fluoride and arsenic from the Independence Aquifer groundwater in Guanajuato, Mexico. Six experiments were conducted to define and model adsorbent performance. The adsorbents tested included locally produced BC, both untreated and acetic acid treated, for fluoride and commercially produced arsenic adsorbents: Bayoxide ® E33, Bayoxide ® E33 HC, and TiO_2 granular media suspended in sand. The feed water of the experiment consisted of local groundwater of 40 μg/L and 8.5 mg/L arsenic and fluoride concentrations

respectively. The filter treatment objective is based on the WHO potable water concentration limits of 10 μg/L and 1.5 mg/L for arsenic and fluoride respectively. Each experiment had specific objectives aimed at contributing to the final filter design by improving BC production, determining the best commercial arsenic adsorbent available, and modelling a continuous BC fixed bed adsorption system performance.

A batch test, experiment 4.1.1, ensured that variation in pyrolysis time during BC production did not affect its fluoride adsorption capacity. Five separate batches of BC were charred by being maintained between 400-600°C for 1, 1.5, 2.5, 4, and 5.5 hours respectively. The adsorption capacities of the different batches all tested within 2% except for the 0.2 g adsorbent dose which tested with a greater variation due to higher errors in fluoride measurements, as explained in Section 4.1.1. The experiment, therefore, confirmed that varying pyrolysis duration does not affect adsorption capacity. Results from a 24-hour kinetic test and a one week long batch test (experiments 4.1.2 and 4.1.3) indicated that Bayoxide ® E33 has a significantly higher adsorption capacity to arsenic in the local groundwater chemistry compared to other commercial adsorbents tested.

Continuous fixed bed experiments were conducted to test the BC's fluoride adsorption capacity. Adsorption capacities were compared between acid treated BC and untreated BC in experiment 4.2.1; the adsorption capacities calculated were 6.2 ± 0.4 mg/g and 5.5 ± 0.3 mg/g respectively. Although acid treated BC tested with a greater adsorption capacity; a decision to use untreated BC for the final design was taken. Because of the particular filter application, which will be in rural locations without easy maintenance access, maintaining system simplicity and avoiding chemical addition within the design was deemed more beneficial than the small adsorption capacity increase of acid treated BC. Using reverse osmosis treated water as a carrier, experiment 4.2.2 investigated regeneration of BC. Only 50 % of fluoride was removed after passing 767 L of carrier through the saturated BC column. Reverse osmosis treated water was concluded not to be an effective carrier for regeneration due to its lack of efficiency and energy intensive treatment. Lastly, variation of empty bed contact time for untreated BC was tested in experiment 4.2.3; decreasing empty bed contact time resulted in a decrease in adsorption capacity. This experiment's results did not offer very reliable results but did suggest that the BC fluoride adsorption operates under equilibrium control and that running fixed beds at the lowest flowrate possible is better for both adsorption capacity and flowrate control.

6.2 Experimental Recommendations Summary

Section 5, the critical analysis, discusses recommendations based on the theoretical basis summarised by section 2 and the specific design requirements and priorities of the project. The experiments summarised in section 4 of this report indicate that the best current commercial adsorbent available is Bayoxide ® E33 for arsenic ions and that the locally produced untreated BC is the best adsorbent for fluoride ions.

To improve the encountered experimental issues, a number of improvements and further experimental investigation are suggested. For the flowrate control failures, inserting a level control to the feed storage unit, operating at the lowest flowrate possible based on the capacity needed, and introducing stabilising media within the fixed bed to ensure stability and homogeneity of bed void fraction are all possible solutions and system improvements. The experiment suggested in Section 5.1.1 of the critical analysis will further ensure temperature variations do not significantly affect adsorption success. Laslty, insulating the feed storage unit in the first pilot will avoid the introduction of another variable for future experiments.

Although the solutions to more advanced and inexpensive arsenic test kits are essentially non-existent, Caminos de Agua has decided to more frequently validate results obtained through university and laboratories with access to and atomic absorption spectrometer. Lastly, there would be value in conducting a more in-depth error analysis, including standard deviation calculations and random error estimations, due to the apparatus errors observed.

Acknowledgments

I would like to thank Engineers without Borders UK for selecting and training me for this research placement, and my academic supervisor, Dr. Enzo Mangano, for making time to patiently answer my every query. Above all, my gratitude goes to the Caminos de Agua team; working within this inspiring group changed me for the better.

References

AdEdge Technologies Inc., 2011. *Bayoxide® E33 Adsorption Media – Arsenic Reduction,* Buford: s.n.

Barros, M., Arroyo, P. A. & Silva, E. A., 2013. General Aspects of Aqueous Sorption in Fixed Beds. *InTech,* pp. 361-383.

Bissen, M. & Frimmel, F., 2003. Arsenic - a Review. Part I: Occurence, Toxicity, Speciation, Mobility. *CLEAN - Soil, Air, Water,* 8 July, 31(1), pp. 9-18.

Bissen, M. & Frimmel, F., 2003. Arsenic - a Review. Part II: Oxidation of Arsenic and its Removal in Water Treatment. *CLEAN Soil, Air, Water,* October, 31(2), pp. 97-107.

Caminos de Agua, 2017. *Optimizing fluoride adsorption and removal using bone char in a lead-lag column configuration,* San Miguel de Allende: s.n.

Caminos de Agua, 2018. *Ensuring safe, healthy, and accessible drinking water.* [Online] Available at: https://caminosdeagua.org/en/home/ [Accessed 8 April 2018].

Chen, Y.-N., Chai, L.-Y. & Shu, Y.-D., 2008. Study of arsenic(V) adsorption on bone char from aqueous solution. *Journal of Hazardous Materials,* Volume 160, pp. 168-172.

Chibi, C. & Haarhoff, J., 2000. *Promising Approach to Fluoride Removal in Rural Drinking Water Supplies,* Sun City: WISA Biennial Conference.

Cunningham, R. E. & Williams, R. J. J., 1980. *Diffusion in Gases and Porous Media.* 1st ed. Boston: Springer.

Donohue, M. D. & Aranovich, G. L., 1998. Classification of Gibbs Adsorption Isotherms. *Advances in Colloid and Interface Science,* pp. 137-152.

Eikelboom, M., 2017. *Developing a low-cost filter medium for remedation of arsenic in contaminated groundwater,* San Miguel de Allende: s.n.

Engineers without Borders UK, 2017. *Who we are. Our Story..* [Online] Available at: https://www.ewb-uk.org/who-we-are/our-story/ [Accessed March 2018].

Fan, X., Parker, D. & Smith, M., 2003. Adsorption kinetic of fluoride on low cost materials. *Water Research ,* pp. 4929-4937.

Hach, 2017. *Pocket Colorimeter™ II, Fluoride.* [Online] Available at: https://www.hach.com/pocket-colorimeter-ii-fluoride-spadns/product-downloads?id=7640445204 [Accessed 12 April 2018].

Han, R., Wang, Y., Zhao, X. & Wang, Y., 2009. Adsorption of methylene blue by phoenix tree leaf powder in a fixed-bed column: experiments and prediction of breakthrough curves. *Desalination,* Issue 245, pp. 284-297.

Helfferich, F., 1995. *Ion Exchange.* 1st Edition ed. New York: Dover Publications, Inc .

Hering, J. G., Katsoyiannis, I. A., Theoduloz, G. & Berg, M., 2017. Arsenic Removal from Drinking Water: Experiences with Technologies and Constraints in Practice. *Journal Environmental Engineering,* 143(5), pp. 1-9.

Hobson, O. & Terrel, D., 2015. *Low-tech gasifiers for production of bone char as a low-cost filter media for fluoride reduction in contaminated groundwater,* San Miguel de Allende: CATIS Mexico.

Huggins, T. et al., n.d. Biochar as a sustainable electrofde material for electricity production in microbial fuel cells. *Bioresource Technology.*

Kearns, J., 2012. *Fabricating a 200 liter biomass gasifier for making enhanced water filter biochar,* Thailand: Aqueous Solutions.

Lanxess, 2018. *Bayoxide E33 HC.* [Online] Available at: http://bayferrox.com/en/products-applications-bfx/product-search/bayoxide-e-33-hc/ [Accessed 12 April 2018].

Lin, T., Liu, C. & Hsieh, W., 2006. Adsorption kinetics and equilibrium of arsenic onto an iron-based adsorbent and an ion exchange resin. *Water Science & Technology: Water Supply,* pp. 201-207.

Loebenstein, W. V., 1962. Batch Adsorption From Solution. *Journal of Research of the National Bureau of Standards,* 7 August, 66A(6), pp. 503-515.

Matthews, W. G., Bridgewater, N. J., Sicard, J.-P. & Anderson, R. A., 1983. *Liquid Adsorption Process and Apparatus.* United States, Patent No. 4,372,857 .

Medellin-Castillo, N. A. & et.al., 2014. Adsorption capacity of bone char for removing fluoride from water solution. Role of hydroxyapatite content, adsorption mechanism, and competing anions.. *Journal of Industial and Engineering Chemistry,* pp. 4014-4021.

Medellin-Castillo, N., Leyva-Ramos, R., Ocampo-Perez, R. & Garcia de la Cruz, R., 2007. Adsorption of Fluoride from Water Solution on Bone Char. *Industrial Engineering Chemistry Research,* 22 November.pp. 9205-9212.

Perry, R. H. & Green, D. W., 2008. *Perry's Chemical Engineers' Handbook.* 8th Edition ed. New York: McGraw-Hill.

Radke, C. J. & Prausnitz, J. M., 1972. Adsorption of Organic Solutes from Dilute Aqueous Solution on Activated Carbon. *Industrial Engineering Chemistry Fundamentals,* 11(4), pp. 445-451.

Rodrigues, A. E., LeVan, D. M. & Tondeur, D., 1988. *Adsorption: Science and Technology.* 1st ed. Vimeiro: Kluwer Academic Publishers.

Ruthven, D. M., 1984. *Principles of Adsorption and Adsorption Processes.* New York: John Wiley & Sons.

Smedley, P. L. & Kinniburgh, D. G., 2013. Arsenic in groundwater and the environment. In: O. Selinus, et al. eds. *Essentials of Medical Geology.* s.l.:s.n., pp. 271-310.

Sposito, G., 1998. On points of zero charge. *Environmental science and technology,* 32(19), pp. 2815-2820.

Sundaram, C., Viswanathan, N. & Meenakshi, S., 2008. Uptake of fluoride by nano-hydroxyapatite/chitosan, a bioinorganic composite. *Bioresource Technology,* pp. 8226-8230.

WHO, 2001. *Water-related diseases.* [Online]
Available at: http://www.who.int/water_sanitation_health/diseases-risks/diseases/fluorosis/en/
[Accessed April 2018].

World Helath Organisation, 2008. *Guidelines for drinking-water quality,* Geneva: WHO Library Cataloguing-in-Publication Data.

Appendix A: Detailed Methodologies

Appendix A.1: Adsorbent Production

A.1.1 Bone Char Production

Materials: 200L biomass gasifier, animal bones, ~50 L water, collection bag, temperature probe

1. Cut bones in pieces of around 5 cm in length
2. Fill the 200L reactor body of the biomass gasifier with bones pieces;
3. Light a fire on top of the bones and carefully place the chimney on the reactor body;
4. Wait until the pyrolysis is completed, this is ensured by waiting for the bones to be between 400 C and 600°C for 1.5 hours (For experiment 4.2.1 the time per. Pyrolysis is done when all biomass is charred, the fire will turn from normal campfire color to pale blue;

5a. Take off the chimney and pour water over the char and the reactor body to stop burning and lower the temperature. Afterwards the char can be collected right away in a bag.
Or
5b. Take off the chimney and put a lid on the reactor body and make it airtight with mud to stop the burning. After 12 hours, the char will be cooled down a ready to collect.

A.1.2 Reverse Osmosis Flushing Bone Char – Phosphate Leaching

Materials: Pre-sieved bone char, number 30 sieve, RO water, column and column system.

1. Weigh the pre-sieved bone char (dry weight).
2. Take pre-sieved bone char and sift it through number 30 sieve with RO water until no additional bone char comes through sieve.
3. Pack wet char inside the inner column cartridge.
4. Screw the outer column cartridge closed around inner cartridge.
5. Attach inlet tube of column system to RO tap.
6. Attach outlet tube to an empty waste container.
7. Attach column to column system.
8. Weigh each dry container for dry weight.
9. Start RO flow.

10. Sample inlet and outlet water using sample bags at time 0 hours and following every hour until fluoride concentration at the inlet is equal to the concentration at the outlet.
11. At each sampling time, weigh the container full of water, empty the water, and weigh the empty container.

A.1.3 Acid Treatment of Bone Char
Materials: Acetic Acid, Bone Char, deionised (DI) Water, container, oven, thermocouple

1. Fill Container with acetic acid
2. Soak bone char in the acid within the container, and leave for 72 hours
3. Sieve bone char out of acid
4. Dry in an over with a thermocouple while monitoring the temperature
5. Rinse bone char with DI water
6. Repeat step 4

Appendix A.2 Batch Experiments

A.2.1 24 hour kinetic experiments

a. Commercial Arsenic Adsorbents
Materials: TiO_2, Bayoxide E33, Bayoxide E33 HC, carat scale, 100mL sealable test tubes, tumbler, As test kit, pH probe, TDS probe, plastic bag, scissors, rubber bands, Teflon tape.

1. Tare the carat scale with the weighing tin on the scale.
2. Weigh out 0.005 grams of the first commercial As adsorbent.
3. Place the material in a sealable 100mL container.
4. Write down the mass of the sample and the sample bottle's number.
5. Repeat steps 2-4. This is your sample duplicate.
6. Repeat steps 2-5 for the following masses (grams): 0.01, 0.05, 0.1.
7. Set aside two additional containers for blanks.
8. Record all sample information (mass, material, bottle number).
9. Weight sample bottle with dry adsorbent.
10. Fill each sample bottle with 90 mL of contaminated water by measuring out 10 mL of water nine times using the pipette.
11. Weigh each sample bottle and subtract dry weight to record water weight.
12. Test each filled tube for leaking. If the tube is leaking, it can be sealed by removing the lid, placing a square (approximately 20cm x 20cm) of plastic bag on top of the tube, and wrapping a rubber band around the tube and plastic three times. Alternatively an O-ring can be created out of Teflon tape. Roll the Teflon into a thin strip and insert it into the innermost ring of the lid.

13. Place the bottles in the tumbler and tumble the samples for 24 hours.
14. Test the As, pH, and TDS of the sample water at the start of the experiment.
15. After 24 hours remove the sample bottles from the tumbler.
16. Test each sample for As, pH, and TDS.
17. Record data.

b. Bone Char Batches

Materials: Various Bone Char batches, carat scale, 100mL sealable test tubes, tumbler, fluoride colorimeter and reagent, pH probe, TDS probe, plastic bag, scissors, rubber bands, Teflon tape.

18. Tare the carat scale with the weighing tin on the scale.
19. Weigh out 0.2 grams of the first commercial As adsorbent.
20. Place the material in a sealable 100mL container.
21. Write down the mass of the sample and the sample bottle's number.
22. Repeat steps 2-4. This is your sample duplicate.
23. Repeat steps 2-5 for the following masses (grams): 0.5, 1, 1.5
24. Set aside two additional containers for blanks.
25. Record all sample information (mass, material, bottle number).
26. Weight sample bottle with dry adsorbent.
27. Fill each sample bottle with 90 mL of contaminated water by measuring out 10 mL of water nine times using the pipette.
28. Weigh each sample bottle and subtract dry weight to record water weight.
29. Test each filled tube for leaking. If the tube is leaking, it can be sealed by removing the lid, placing a square (approximately 20cm x 20cm) of plastic bag on top of the tube, and wrapping a rubber band around the tube and plastic three times. Alternatively an O-ring can be created out of Teflon tape. Roll the Teflon into a thin strip and insert it into the innermost ring of the lid.
30. Place the bottles in the tumbler and tumble the samples for 24 hours.
31. Test the Fluoride, pH, and TDS of the sample water at the start of the experiment.
32. After 24 hours remove the sample bottles from the tumbler.
33. Test each sample for Fluoride, pH, and TDS.
34. Record data.

A.2.1 1 week batch experiments

Materials: TiO_2, Bayoxide E33 HC, carat scale, 100mL sealable test tubes, tumbler, As test kit, pH probe, TDS probe, plastic bag, scissors, rubber bands, Teflon tape.

1. Tare the carat scale with the weighing tin on the scale.
2. Weigh out 0.005 grams of the Bayoxide E33 HC adsorbent.
3. Place the material in a sealable 100mL container.

4. Write down the mass of the sample and the sample bottle's number.
5. Repeat steps 2-4 until you have 22 bottles with Bayoxide E33 HC.
6. Weigh out 0.08 grams of the TiO_2 adsorbent.
7. Place the material in a sealable 100mL container.
8. Write down the mass of the sample and the sample bottle's number.
9. Repeat steps 6-8 until you have 22 bottles with TiO_2 adsorbent.
10. Set aside six additional containers filled with sample water for blanks.
11. Test each filled tube for leaking. If the tube is leaking, it can be sealed by removing the lid, placing a square (approximately 20cm x 20cm) of plastic bag on top of the tube, and wrapping a rubber band around the tube and plastic three times. Alternatively an O-ring can be created out of Teflon tape. Roll the Teflon into a thin strip and insert it into the innermost ring of the lid.
12. Place the bottles in the tumbler and tumble the samples. Take out two samples of Bayoxide E33 HC and two samples of TiO_2 adsorbent after 0, 0.25, 0.5, 1, 1.5, 3, 6, 12, 24, 72, and 168 hours. Take out two samples of blank after 0, 72, and 168 hours.
13. Filter each sample immediately after removing it from the tumbler using a coffee filter.
14. Test each filtered sample for As, pH, and TDS.
15. Record data.

Appendix A.3 Column Experiments

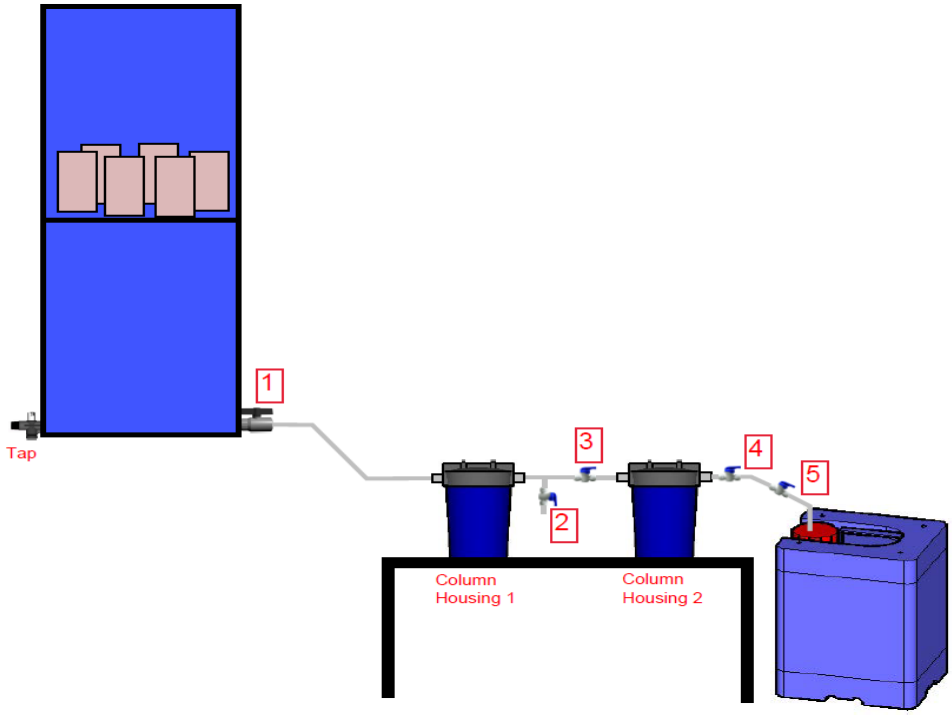

Figure 29: Column Set Up Diagram

I. *Preparation of influent water*

Sample water protocol:

1. Mix community water (>8mg/L of fluoride) in cubo with an electric paint mixer for 10 minutes before taking at least 2 samples to establish the average fluoride concentration. The fluoride samples should not differ >0.5mg/L from one another. If this is not the case, mix the water for a further 5 minutes and repeat the step until all measurements are within a 0.5mg/L range.
2. Test a sample of household water (<8mg/L of fluoride) within 30min of diluting the cubo water in order to establish the quantity of water needed for dilution. *Note: this should be done at the location where the dilution will take place.*
3. Calculate the quantity of household water required to dilute the community water to achieve a concentration of approximately 8.25mg/L.
4. Dilute the community water in the Cubo with the calculated quantity of household water.
5. Mix for 10 minutes with an electric paint mixer.
6. Test a sample from the top of the Cubo and the bottom. If both samples measure between 8mg/L to 8.5mg/L of fluoride follow step 6. If both samples do not measure between 8mg/L to 8.5mg/L, mix the water for a further 5-10 minutes with the electric paint mixer. Repeat this step until both samples measure between 8mg/L to 8.5mg/L of fluoride.
7. Fill a minimum of 6x20L jerry cans with the diluted community water. This will only be enough for 1 day at the appropriate flow rates with 4 column set-ups running.
8. Every time more water is needed and jerry cans need to be filled, repeat steps 5-6.
9. NOTE: For baselines, just use hose to connect RO effluent to inlet water storage upstream of columns.
10. *Pre-start and start of column test*
11. Preparing the filter cartridges:
12. Fill two empty cartridge filters with the appropriate char as much as possible. The char should be about half a cm from the top of the cartridge.
13. Close the filters and compact the char by shaking them thoroughly for roughly 30 seconds.
14. Reopen the filters and add more char to within a few mm from the top.
15. Weigh the full cartridge filters to check they are roughly the same. If not, try to compact the lighter filter further by shaking and add more char. It is important not to break the grains of char, so do not compact the filter by hand. Shaking should suffice. Then weigh again. Repeat this until the cartridge filters weigh roughly the same.
16. Make a note of the weights and place the cartridges into the column housings.
17. Connect the column housings to the set-up.
18. Label the first column, closest to the influent water, “column 1.” Label the second column, closest to the effluent, “column 2.”

II. Running the column tests:

NOTE: Refer to Figure 29 for valve labels

1. Before starting a column test with new char, baselines need to take place by running RO through the system. This also has the additional advantage of settling the char which is needed even if baselines do not need to take place.
2. Ensure that for each column set-up: valves 1, 2 and 4 are closed and that the tap on the container is closed.
3. Open the tap on the tub until as much water as possible is drained. Scoop out any remaining water by tilting the tub.
4. Close the tap on the tub, secure its lid
5. Fill the upper container with RO water.
6. With the electric mixer, mix the water for 30 seconds and then take a pre-column filter sample following the instructions under the 'taking samples' section.
7. Whilst waiting 30min until the following step, weigh each container that will be receiving flow from the column set-ups.
8. For each set-up, open valve 1, ensuring that valves 2, 3 and 4 are open. Valve 5 should be partially open or open to allow water to flow through.
9. As soon as water flows out the tube, close valve 4.
10. Press down on the red button on the top of column housing 2 to release air.
11. Without reopening valve 4, press down on the red button every few minutes to release air that is inside the column. Repeat this step until water is released.
12. When water is released upon pressing the red button, close valve 3.
13. Apply steps 12 & 13 to column housing 1 without adjusting any valves.
14. When water is released upon pressing the red button on column housing 1, open valve 3 and valve 4 so that flow enters the containers and make a note of the time.
15. Determine the flow rate of the column set-up and adjust valve 5 until a flowrate between the range of 25.5 ml/min and 27.5 ml/min is measured for set up 1; and 34.5 ml/min and 36.5 ml/min for set up 2. Tip: this flowrate will typically occur when the valve is over half way closed therefore a good starting point is to set valve 5 to approximately half way closed and adjust accordingly from there.

III. *Taking samples*

i. Pre-column samples:

1. A pre-column sample should be taken every time the large upper tub is filled with water as detailed in the following procedure.
2. Label a sample bag with the corresponding code (01 for a pre-column sample, followed by the correct letter) and the date. Instructions on how to label sample bags can be found on tab "Sampling Timetable" in the data collection spreadsheet.
3. Fill the large upper tub to the top and mix for 30 seconds using the electric paint mixer.
4. Scoop enough water from the tub to fill ¾ of the bag, then close.

5. Weigh the bag and write the weight on the bag.
6. The final label on the bags should be as follows: LABELCODE - DATE – WEIGHT e.g. 32C - 17/3 - 198
7. Column samples:
8. As soon as the correct flowrates for each column set-up have been achieved, the first set of samples can be taken. However, the total volume of water passed through each column should be captured in each set-ups' respective containers while trying to achieve this flow.
9. Samples should be taken from column 1 first, then 2.
10. Label all sample bags with the corresponding code and the date. Instructions on how to label sample bags can be found on tab "Sampling Timetable" in the data collection spreadsheet.
11. Prepare the corresponding sample bags for columns 1 on the hooks and place them over valve 2 for each respective set-up. The outlet of the tube from valve 2 should be positioned in the sample bag.
12. For each set-up, operate the valves as follows: close valve 4 followed by valve 3 so that no air gaps are formed. Make a note of the time to enter into the data collection spreadsheet afterwards.
13. Consecutively for each set-up, open valve 2 as slowly as possible until the flow rate appears similar to that which flows out of column 2 (no flow should be coming from column 2 at this time).
14. While the sample bags are filling, weigh the containers in the same order that valves 2 were operated in order to ascertain how much water has passed through the columns since the last sample was taken. *Note: it may be safer to take samples from two set-ups at a time (rather than all 4) so that there is sufficient time to measure the containers before the sample bags are full. This will depend on the amount of time since the last sample was taken, and the capacity of the scale.*
15. Weigh the empty container (to deduct from the volume weight at the next sampling time) and place back under the outlet of its corresponding set-up.
16. Place the pre-labelled sample bag for column 2 of the corresponding set-up into the opening of the jerry can whereby the handles of the bag are sitting over the edge.
17. When the sample bags are ¾ full from column 1, operate the valves in the following order: close valve 2, open valve 3, open valve 4. Ensure that the outflow is going directly into the sample bag for column 2.
18. Carefully remove the bag and hook from valve 2 and close the bag.
19. Repeat this procedure for each set-up.
20. When all samples have been taken, weigh the bags and write the weights on the bags.

Appendix B: Feed Water Chemistry Information

Table 22: Information on test water originated from a well at the Ex-Hacienda de Jesus community

	Ex-Hacienda de Jesus		WHO Guidelines
Date	13-3-2013	19-5-2014	2011
Well depth (m)	275		
Coliform (MPN/100mL)		<1	
E. coli (MPN/100 ml)		<1	
Water Temp (°C)		43.6	
pH	8.61	8.42	
Electronic Conductivity (mS/cm)		579	
Alkaninity (mg/L)		n/d	
Fluoride (mg/L)	16	17.2	1.5
Nitrate (mg/L)		1.18	50
Phosphate (mg/L)		0,2	
Turbidity (NTU)		<2	
Sulfate (mg/L)		63	No health concerns
Arsenic (ppb)	47	60	10

Appendix C: Roles and Responsibilities

I arrived at Caminos de Agua as Experiment 4.2.1 had already been designed and started by previous EWB-UK volunteer, Sarah Mitchell. For this experiment, I started sampling the columns, preparing feed water, and testing water samples roughly 10 days into the experiment and finished it as well as created the graphs and conducted all the error analysis. All other experiments presented in this report were started and executed by me, in collaboration with Caminos de Agua volunteer Sarah Hartman for experiments 4.1.2, 4.1.3, and 4.2.3. On top of the experiments presented I completed the work presented in Appendix D, travelled to rural communities twice to support Caminos de Agua work, and contributed to brainstorm sessions within the organisation's weekly meetings. All the work I conducted was supervised by Aaron Krupp – Caminos de Agua's Research and Technology Development Coordinator.

Appendix D: Hach and ITS Arsenic Field Test Kits Analysis

CAMINOS DE AGUA

Low-cost arsenic testing in natural groundwater: reagent and method validation

An investigation into the accuracy and reliability of commercial arsenic field test kits and appropriate validation methods

Prepared by: Caminos de Agua
October 30, 2017

1

TABLE OF CONTENTS

ACKNOWLEDGEMENTS

Caminos de Agua would like to sincerely thank the **Natural Health Research Foundation** and **Dr. Mercola** for their continued support of research aimed at spreading and allowing safe and healthy water usage and consumption practices. Without this support — and the freedom to explore unique solutions and follow the research where it leads us — none of this work would be possible.

This particular research effort was supported with conversations, feedback, and guidance by a number of academic and industry colleagues including Matthew Polizzotto (University of Oregon); Kevin Plaxco, Netz Arroyo, Aaron Rowe (University of California -- Santa Barbara); Yanmei Li (University of Guanajuato); Channa Jayasumana (Rajarata University of Sri Lanka); Ralf Cord-Ruwisch, Hans Oskierski, Mahamudul Hassan (Murdoch University); Peter Knappett (Texas A&M University); and Maisie Mahoney (Merck). A special thank you to **Dr. Joshua Kearns** of North Carolina State University for providing unparalleled technical guidance.

We thank **Ecolaboratorios**, the independent laboratory that analysed a variety of samples with AAS, allowing this research to be completed.

Finally, an enormous THANK YOU! to **Martijn Eikelboom** of Van Hall Larenstein University and Wageningen University for first discovering this issue and **Simona Dossi** of Engineers Without Borders UK for battling with these test kits and preparing this report.

ABSTRACT

In April 2017, Caminos de Agua received a batch of Hash EZ Arsenic Test Kit reagents used to measure arsenic in potable water. The results were dramatically different than expected. This led to an investigation of the accuracy and replicability of results from two brands of arsenic field test kits: Hach's EZ Arsenic Test Kits and Industrial Test System's (ITS) Quick Kits. Prepared standard solutions and various groundwater samples were tested with reagent combinations from both kits and validated against an independent laboratory's atomic absorption spectrometer (AAS). This study concludes that ITS's kits are more accurate and reliable than Hach's for natural waters of the Independence Watershed. For eleven out of thirteen samples tested — ranging from 1 to 250 µg/L — the ITS kits were within ±5 µg/L of the AAS result. All but one sample tested with the Hach kits exceeded this error margin. These results led Caminos de Agua to exclusively use ITS's Quick Kits for arsenic testing, accompanied by regular kit validation with AAS.

1. INTRODUCTION

1.1 Caminos de Agua's dependence on arsenic field test kits

Caminos de Agua depends on low-cost aqueous arsenic field test kits for two crucial projects:

(1) regional water quality monitoring and
(2) research and development of filters that adsorb arsenic and fluoride from groundwater.

The water quality monitoring project allows Caminos de Agua to map regional tap and well quality by testing samples from around central Mexico's Independence Watershed for fluoride and arsenic contamination. This is a crucial tool used to inform the public about about regional water quality and to track changing contamination levels. Caminos de Agua has also been conducting promising research aimed at developing low-cost adsorption filters for fluoride and arsenic removal from regional groundwater. Numerous batch and column experiments are conducted to advance this exciting project. Caminos de Agua, therefore, depends on accurate, affordable arsenic testing methods to monitor contamination and develop appropriate solutions.

For field test kits to be useful for Caminos de Agua's work, they need to produce results within a consistent error range. For private water quality testing, communities and customers want to

know whether their water falls above the World Health Organization's limit of 10 µg/L. Therefore, for results below 25 µg/L, Caminos de Agua requires an accuracy of ±4 µg/L. For filter development, Caminos de Agua measures reductions from 80 to below 10 µg/L. For the higher ranges, above 25 µg/L, Caminos de Agua needs a minimum accuracy of ±20% to accurately assess removal. These threshold values are summarized in table 1.1. This report uses these error values to assess the quality of the field test kits for practicality. In this investigation, the samples will be divided by concentration (above or below 25 µg/L) based on the test kits results. This approach was selected because Caminos the Agua cannot realistically check sample concentrations with an AAS, therefore, decisions need to be based on test kits' results.

Water Arsenic Concentration	< 25 µg/L	≥ 25 µg/L
Minimum Acceptable Accuracy	±4 µg/L	±20%

Table 1.1: *Caminos de Agua acceptable arsenic concentration error for water samples.*

1.2 History of arsenic field testing uncertainties

Caminos de Agua has used Hach's EZ Arsenic Test Kits for five years of active research and water quality monitoring with regularly validated results in accredited laboratories. Collaborators at Texas A&M University tested six water samples perviously tested by Caminos de Agua with arsenic field tests in August 2016 (Thurston, 2016); from the results it was concluded the error in the arsenic field test results for these samples was no greater than ±4.7 µg/L. In April 2017, a newly purchased batch of Hach's reagents were used for testing. They gave unexpected results for samples of natural groundwater of known concentration. After this incident, while waiting for replacement reagents from Hach, Caminos de Agua purchased an ITS QuickTest Field Arsenic Kit. These kits were used until the new batch of Hach reagents arrived. In June, 2017, the new Hach reagents again gave unexpected results. A third batch of replacement reagents of the faulty kits were provided by Hach in September, 2017, along with a standard concentrated solution of 1000 mg/L arsenic. In September, both Hach and ITS kits were used to test the same sample and gave different values. These unexpected and contradictory results caused grave concern regarding the reliability of Caminos de Agua's aqueous arsenic testing. Unreliable testing not only affects the organization's laboratory results but also impacts people

who rely on Caminos de Agua to determine whether their water is safe to consume. The following report details the organization's attempt to quantitatively validate both kits.

2. MATERIALS AND METHODS

To quantitatively validate the two test kits, standard solutions of arsenic were prepared by diluting the 1000 mg/L Hach arsenic concentrate, natural aqueous stabilisation practices (refrigeration, obscuration of sunlight, and acidification) were researched (summarised in section 4.3), and various groundwater samples were sent to be tested by AAS at an independent laboratory. Percent and absolute errors were calculated between each test kit and the AAS results. The following section summarises test methodologies; for step-by-step protocols, refer to Appendix A.

2.1 Arsenic standard solution preparation

The Hach 1000 mg/L Arsenic concentrated solution was diluted with deionized water to create standard solutions with concentrations of 80, 150, 250, and 500 µg/L.

2.2 Acid stabilization of aqueous arsenic samples

One natural water sample was acidified to below pH 2 using 4.5 M HCl solution. A natural water sample containing arsenic was divided in two equal volumes (400 ml). One was left unchanged while the other was lowered to pH = 1.9.

2.3 Field test aqueous arsenic method

For both ITS and Hach test kits, the commercial instructions provided were followed (see Appendix A.3.1 and A.3.2 respectively for details).

2.4 Hach and ITS field test kit information

Company: Hach
Name: EZ Arsenic Test Kit
Method of Arsenic Test:
Reagents include sulfamic acid, zinc, and mercuric bromide strips. The contaminated water sample produces arsine gas (AsH_3) when zinc (Zn) is added. The EZ kit relies on sulfamic acid crystals to acidify the sample in order to eliminate interference by hydrogen sulfide. The kit

correlates to arsenic concentration in water samples using Gutzeit Reaction - the reaction between $HgBr_2$ and AsH_3 which produces a colour change (George, 2012).

Detection Range [µg/L] : 0, 10, 25, 50, 100, 250, 500

Figure 2.1: *Hach EZ Arsenic Test Kit components.*

Company: Industrial Test Systems
Name: Inorganic Quick™ Arsenic Test Kits
Method of Arsenic Test:
Inorganic arsenic compounds are converted to arsine gas (AsH_3) by reaction of zinc and tartaric acid. Ferrous and nickel salts have been added to accelerate the reaction. Potassium peroxymonosulfate is also added to the sample to convert hydrogen sulfide to sulfate. The test strips contain mercuric bromide ($HgBr_2$) and the arsine gas reacts with it to generate mercury halogens that produce a colour change (Gutzeit Reaction); as described in the kit instruction manual (ITS, 2016).

Detection Range [µg/L] : 0, 3, 5, 7, 8, 9, 10, 12, 16, 20, 25, 30, 40, 50, 80, >80, >90, >100

Figure 2.2: *ITS QuickTest Field Arsenic Kit components.*

3. RESULTS

3.1 Independent laboratory's AAS results comparison

The final comparison data between the AAS and field test kits results is presented for the ITS and Hach kits in table 3.1 and table 3.2 respectively, along with real and absolute percent errors

3.2 Outlier natural water sample and acidification results

The only water sample with arsenic concentration greater than 25 µg/L that yielded more than a 20% error with the Quick ITS tests was Well Water 1 (see table 3.1); this sample was kept -- unstabilised -- for over six months in a sealed by not-air-tight plastic jerrycan. In the forthcoming analysis, this outlier was ignored. Research regarding laboratory stabilisation efforts (see section 4.3) was conducted to understand why both test kits consistently yielded incorrect results for this sample. Furthermore, to test the effect of sample acidification on total aqueous arsenic, the two identical samples described in section 2.2 were tested with AAS. The results are summarised in table 3.3. The samples were both tested 7-10 days after acidification.

3.3 Distribution of error

Excluding the outlier sample (well water 1), from the errors measured due to its significantly larger error and different water conditions, a statistical analysis was conducted on the errors. Figure 3.1 and 3.2 show the distribution around zero of the real errors for samples of arsenic concentration < 25 µg/L, and percent errors for samples of arsenic concentration ≥ 25 µg/L respectively.

Expected Concentration/ Description	AAS Result	ITS Kit Result	Error	Percent Error
	µg/L	µg/L	µg/L	%
Standard Solution 2 - 250 µg/L	177.7	>100	/	/
Standard Solution 3 - 150 µg/L	29.4	25	-4.4	-14.97
Standard Solution 4 - 80 µg/L	61.8	50	-11.8	-19.09
Standard Solution 5 - 80 µg/L	73.7	80	6.3	8.55
Well Water 1	70.7	37.29*	-33.41	-47.26
Well Water 2	25.3	25	-0.3	-1.19
Well Water 3	11.3	12	0.7	6.19
Well Water 4	25	20	-5	-20
Tap Water 1	9	7	-2	-22.22
Tap Water 2	13	18	5	38.46
Tap Water 3	7.4	3	-4.4	-59.46
Tap Water 4	8.2	3	-5.2	-63.41

Table 3.1: ITS Field Test Kit and AAS Results Comparison

Values marked by asterisks (*) indicate an average of multiple tests. Percent error is colored if the test value is ≥25 µg/L. Error is colored if the test value is <25 µg/L. Percentage errors are marked red if greater than 20% and green otherwise. Absolute errors are marked red if greater than 4 µg/L, and green if lower than 4 µg/L.

Figure 3.1 shows that although the sample sizes of the data are relatively small, the data validates the assumption of normal distribution of errors. In figures 3.1(a) and (b), the normal fit for the ITS data is thinner than the Hach normal fit, visually demonstrating that the ITS tests are less variable than their Hach counterparts. Additionally, both ITS curves are centered near 0 (as

Expected Concentration/ Description	AAS Result	Hach Result: Batch 1	Error	Percent Error	Hach Result: Batch 2	Error	Percent Error
	µg/L	*µg/L*	*µg/L*	%	*µg/L*	*µg/L*	%
Standard Solution 1 - 500 *µg/L*	216.1	200	-16.1	-7.45	200	-16.1	-7.45
Standard Solution 2 - 250 *µg/L*	177.7	100	-77.7	-43.73	90	-87.7	-49.35
Standard Solution 3 - 150 *µg/L*	29.4	20	-9.4	-31.97	20	-9.4	-31.97
Standard Solution 4 - 80 *µg/L*	61.8	50	-11.8	-19.09	25	-36.8	-59.55
Well Water 1	70.7	10*	-60.7	-85.86	10	-60.7	-85.86
Well Water 2	25.3	20	-5.3	-20.95	/	/	/
Well Water 3	11.3	0	-11.3	/	5	-6.3	-55.75
Well Water 4	25	5	-20	-80	10	-15	-60
Tap Water 1	9	0	-9	/	0	-9	/
Tap Water 2	13	2	-11	-84.62	1	-12	-92.31
Tap Water 3	7.4	0	-7.4	/	/	/	/
Tap Water 4	8.2	0	-8.2	/	10	1.8	21.95

Table 3.2: Hach Field Test Kit and AAS Results Comparison

The two different Hach field test kits results for each sample are differentiated by the different batch numbers of reagent 1 used for the tests. The number of each batch is indicated in the headline for the test columns. As in Table 3.1, values marked by asterisks (*) indicate an average of multiple tests. Percent error is colored if the test value is ≥25 µg/L. Error is colored if the test value is <25 µg/L. Percentage errors are marked red if greater than 20% and green otherwise. Absolute errors are marked red if greater than 4 µg/L, and green if lower than 4 µg/L. Percentage errors for kit results that gave 0 µg/L were not calculated as 100 % percentage error would be a misleading value compared to the other percentage errors.

Expected Concentration/Description	AAS Results
	µg/L
Well Water 4	25
Well Water 4 - Acidified	38

Table 3.3: *AAS Results Comparison for acidified and non-acidified natural water sample.*

expected) while the Hach curves are shifted left, indicating that Hach kits tend to yield low results. .

Table 3.4 summarises the sample size, mean average, standard deviation, and confidence interval for the mean of the real errors and percentage errors for both ITS and Hach field kits.

The sample statistics summarised in table 3.4 indicate the ITS kits are more accurate than the Hach kits. Firstly, the mean average errors are smaller (closer to the ideal 0) for the ITS kit. The standard deviation of the errors is also smaller for the ITS kit results, indicating the errors are less varied. Lastly, the 95% confidence intervals for the ITS errors include 0 while for the Hach test they do not; this is strong evidence the Hach kits consistently test below the real concentration of the water sample while the ITS errors are more evenly spread: some low and others high. Noting the small sample size used for

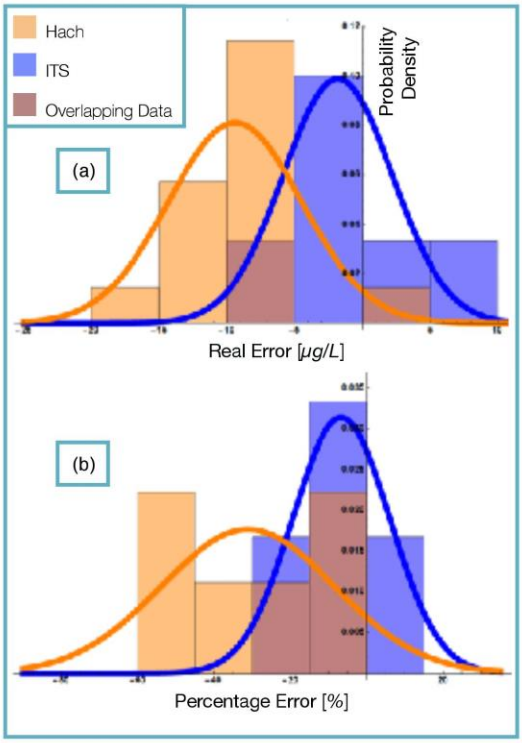

Figure 3.1: *Histogram of ITS and Hach error results for (a) real errors for samples reading below 25 µg/L and (b) percent errors calculated for samples reading 25 µg/L or above. On both graphs probability density is shown on the vertical axis.*

	Real Error (result <25 µg/L)		Percentage Error (results ≥25 µg/L)	
	ITS	Hach	ITS	Hach
Sample size	6	14	4	6
Mean	-1.8	-9.4	-6.7	-31
Standard deviation	4.03	4.92	12.7	22.6
Desired range	±4 µg/L		±20%	
Percentage of data that falls within	63%	13%	83%	30%

Table 3.4: *Sample statistics of errors calculated for ITS and Hach field kits. The desired range comes from section 1.1. The percentages of samples that fall within the desired range are calculated by assuming the normal distributions plotted in figure 3.1 are accurate and calculating probability density at the limiting points.*

these calculations, we acknowledge further investigations with a larger sample size are necessary to confirm our calculations and conclusions.

For the real errors calculated, 30% of the samples tested with the ITS kits had real errors that fell within the acceptable Caminos de Agua error range of ± 4 µg/L, while only 5% of the samples tested with Hach kits had errors within this range. Similarly, for percentage error 60% of samples tested with ITS resulted in errors within the acceptable Caminos de Agua range of ±20% error, while only 3% of samples tested with Hach fell within the acceptable range. However, based on the Gaussian approximation curves shown in figure 3.1, we see that we would expect 63% and 83% of all samples tested with the ITS kits to fall into the appropriate error ranges for low and high samples respectively. The corresponding numbers are much lower, 13% and 30%, for the Hach kits.

4. DISCUSSION

In the following section, the errors presented in section 3 are compared to the minimum accuracy required by Caminos de Agua. As explained in section 1.1, Caminos de Agua requires an accuracy of ±4 µg/L for results below 25 µg/L and ±20% for results above and including 25 µg/L. In this section, therefore, the samples will be divided between samples of

water with a arsenic concentration of <25 µg/L and those with an arsenic concentration of 25 µg/L or above for analysis. Test kit concentrations were used for practicality, since Caminos de Agua cannot verify every sample with AAS and will apply different error margins -- 4 ug/L or 20% -- for samples below or above 25 ug/L respectively. The outlier sample (the well water sample discussed in section 3.2) was excluded from the analysis.

4.1 Samples with arsenic concentration below 25 µg/L

Based on the data shown in table 3.4,
33.3% of ITS tested samples tested within the acceptable error range of ±4 µg/L, while only 8.33 % of samples tested with Hach tested within the acceptable error range. Additionally, the most extreme ITS error on a sample below 25 µg/L as -5.2 µg/L, which is very close to the acceptable range. Using the extrapolated normal distribution pictured in figure 3.1, we predict that 63% of all samples tested with the ITS kits will fall into the appropriate error range, as opposed to only 13% of Each results.

The calculated 95% confidence interval indicates that the true mean error for Hach field test kits is between -11.0 µg/L and -0.6 µg/L. We can say with 95% confidence that the Hach kits test *below* the real water concentration. Furthermore, the errors are spread throughout a large range, indicating unpredictability.

Although these calculations indicate that the ITS field kits test with close to an acceptable error for the organisation's needs, we note that there is a small sample size of only 6 samples. To ensure the calculated error, therefore, Caminos de Agua should conduct a larger statistical investigation.

4.2 Samples with arsenic concentration of 25 µg/L and above

Table 3.4 also shows the sample size, mean, standard deviation, of percent errors of the ITS and Hach field test kits only including samples with arsenic concentrations of 25 µg/L or above. The Caminos the Agua requirement accuracy for this arsenic concentration range in water is ±20%.

Excluding the outlier, all ITS samples tested within the acceptable error range of ±20%, while only 25% of Hach samples tested within the acceptable error range. This is very strong evidence in favour of ITS testing samples with an acceptable error and Hach performing more poorly. Using the extrapolated Gaussian, we predict that 83% of all ITS samples would fall within the range, compared to only 30% for Hach. The sample size for ITS tested sample, however, is even smaller than the one discussed in section 4.1 - consisting of only four samples. To ensure the calculated error, therefore, Caminos de Agua recommends conducting a larger statistical investigation.

The 95% confidence interval for the mean percent error of the Hach kits' results is (-52%, -16%). This shows that for high arsenic concentrations the Hach kits also yield significantly low results. Without further calculations or analysis these data demonstrate that Hach kits yield unacceptably large errors and consistently low results. In comparison, while the ITS results are not exclusively within the stated error bounds they are close and seem to provide an non-skewed error distribution for high and low samples.

4.3 Effect of acid stabilisation

The results of the literature review conducted regarding arsenic stabilisation methods in response to the outlier water sample, Well Water 1, is summarised below. Kumar and Riyazuddin published a comprehensive literature review analysing various published articles regarding preserving inorganic arsenic species in water samples (Kumar, 2010). The methods most widely used to preserve water sample concentrations and water chemistry are filtration, refrigeration, and storage in absence of light. These processes remove suspended matter and the majority of microbes that could cause precipitation or chemical reactions with dissolved solids, slow down or prevent biotic and abiotic reactions, and prohibit photochemical reactions.

The predominant species of inorganic arsenic present in water are As(III) and As(V), other less present species include MMA and DMA, however these occur in concentrations insignificant to Caminos de Agua's work (Kumar, 2010). Preservation efforts of water samples are used to postpone or prevent redox, co-precipitation, hydrolysis, adsorption, biodegradation and photochemical reaction that can result in concentration changes of the water sample over time. For standard solutions of arsenic prepared in distilled water, precipitation, adsorption and biodegration reactions are not expected to be a complication due to the absence of any other substances in the solution. These solutions are therefore expected to maintain stable

concentration for a longer periods of time but should still be kept refrigerated and away from sunlight (Kumar, 2010).
Acidfication of water samples with inorganic arsenic to pH<2 is also used to minimise precipitation, adsorption, and microbial activity as well as to prevent As(III) to As(V) transformation. Since Caminos de Agua uses field test kits that measure the total arsenic concentration of both species, this method is assumed to only be relevant as an effort to minimise precipitation, adsorption, and microbial activity. Efforts to prevent other types of reactions can be taken including filtration, refrigeration, and obscuration from light. As shown in table 3.3, the acidified and non-acidified samples were tested to have 38 µg/L and 25 µg/L arsenic concentration respectively, a 34% decrease. Although this gives weak evidence in favor of a reduction over time of total arsenic in aqueous samples -- which can be preserved by acidification, one sample is not a large enough sample size to reach a conclusion regarding the necessity or effect of acidification. This result has inspired Caminos de Agua's ongoing investigation into the effect of acidification of samples through more rigorous experimentation.

5. CONCLUSION

This report analysed the accuracy of ITS Quick™ Arsenic Test Kits and Hach EZ Arsenic Test Kits based on acceptable error ranges defined by Caminos de Agua based on the organisation's testing needs. These acceptable error ranges are defined and explained in section 1.1 as ±4 µg/L for water sample with arsenic concentrations below 25 µg/L, and as ±20% for waters with arsenic concentrations of 25 µg/L or higher. The Hach EZ Arsenic Test Kits were found to test outside the acceptable error ranges more than the ITS kits. Based on a normal approximation, this study predicts that for low arsenic concentrations (<25 µg/L), ITS kits perform much better with 63% of all results falling within ±4 µg/L of the AAS value compared to Hach's 13%. For high arsenic concentrations (≥25 µg/L), ITS kits also win out with 83% of all results falling within ±20% of the AAS value compared to 30% for Hach. While ITS results tended to be uniformly distributed around 0, Hach results were consistently skewed low. **This investigation suggests that ITS Quick™ Arsenic Test Kits are accurate enough to be the best available option for field testing for Caminos de Agua's technical development and water quality monitoring teams.**

Further statistical analyses with greater sample sizes, however, are recommended to confirm these preliminary results. Furthermore, while using the ITS kits, Caminos de Agua will take into account the kits' inherent errors.

After conducting a literature review, acidification is suspected to be an unnecessary step to prevent oxidation and changes between arsenic species in aqueous samples when other stabilisation practices (refrigeration, obscuration from sunlight) are used because Caminos de Agua measures the total arsenic concentration in samples and doesn't distinguish between As(III) and As(V) species. A more rigorous experiment will be conducted, however, to ensure that not acidifying samples does not result in any significant reduction in total arsenic concentration. Refrigeration, and obscuration of samples, however, are easier and safer stabilisation methods that should be used to ensure minimal changes in water sample chemistry. **Caminos de Agua encourages all other organizations who use arsenic field kits to test water for human consumption to frequently validate their kits against established laboratory protocols.**

6. REFERENCES

George, Christine Marie, et al. "Evaluation of an Arsenic Test Kit for Rapid Well Screening in Bangladesh." Environmental Science & Technology, vol. 46, no. 20, 25 Oct. 2012, pp. 11213–11219., doi:10.1021/es300253p.

ITS Europe . Quick II Rapid Arsenic Test Kit. Quick II Rapid Arsenic Test Kit, ITS, 2016.

Kumar, Ramesh A., and P. Riyazuddin. "Preservation of inorganic arsenic species in environmental water samples for reliable speciation analysis." Trends in Analytical Chemistry, vol. 29, no. 10, Nov. 2010, pp. 1212–1223.

Thurston, William. As and F Comparison. Caminos de Agua. Aug. 2016.

APPENDIX A - DETAILED METHODOLOGIES

A.1 Arsenic standard solution preparation

Materials: 1000mg/L Arsenic standard solution, 100mL glass beaker, 10mL glass graduated cylinder, 1mL glass pipette, 1.5 liter commercial plastic water bottle, DI water, goggles, and plastic gloves.

Notes: Wear protective gloves, goggles, mask, close-toed shoes, and lab coat when handling hazardous concentrations of arsenic. Conduct appropriate dilution calculations before starting experiment and note down volumes needed.

Methodology:
1. Rinse with DI and dry completely the following equipment: glass beaker, graduated cylinder, glass pipette
2. Shake arsenic standard vigorously to mix well
3. Rinse beaker with As standard [5-10mL]
4. Pour 25mL of As standard in beaker
5. Flush pipette completely with As standard from beaker (repeat 2x)
6. Rinse graduated cylinder with As standard from beaker (repeat 1x)
7. Fill the 10mL graduated cylinder with As standard from beaker
8. Fill 400mL of DI into sample bottle
9. While swirling continuously (use a magnetic stir plate if available — if not, a glove-wearing friend swirling the bottom of the bottle until a vortex develops will do), spike the appropriate amount of As standard into sample bottle.
10. Fill sample bottle with remaining amount of DI, as calculated
11. Shake sample bottles for 5 minutes or continue to use magnetic stir bar, if applicable.

A.2 Acid stabilization of aqueous arsenic samples

Materials: 4.5M HCl solution, glass beaker, glass graduated cylinder, glass pipette, pH meter, PPE

Notes: Wear protective gloves,goggles, lab coat, and close-toed shoes when handling hazardous acids.

Methodology:

1. Rinse with DI and dry completely the following equipment: small glass beaker, graduated cylinder, glass pipette
2. Shake HCl solution vigorously to mix well
3. Rinse beaker with HCl solution [5-10mL]
4. Pour 10 mL of HCl solution in beaker
5. Flush pipette completely with HCl solution from beaker (repeat 2x) [3mL]
6. Rinse graduated cylinder with HCl solution from beaker (repeat 1x) [12mL]
7. Fill the graduated cylinder with HCl solution from beaker [10mL]
8. Measure pH of water sample that needs to be acidified and note down result.
9. Using the pipette, add 0.5 ml of HCl solution to water sample
10. Measure pH of water sample, mixing the sample thoroughly
11. Note down pH
12. Repeat steps 9-12 until pH reads < 2.

A.3 Field test aqueous arsenic method

A.3.1 ITS

Materials: ITS Econo II Quick Rapid Arsenic Test Kit
Methodology:

1. To the reaction bottle, slowly add the water sample until the bottom of the meniscus touches the marked line(approx. 50ml).
2. Add 2 pink spoonfuls (leveled) of First Reagent to the Reaction Bottle. Cap securely and shake vigorously for 15 seconds.
3. Uncap the reaction bottle and add 2 red spoonfuls (leveled) of the Second Reagent. Recap securely with the black cap and shake vigorously for 15 seconds.
4. While the rest is incubating for 2 minutes prepare the turret cap by inserting the test strip in the appropriate location.
5. Uncap the reaction bottle and add 2 white spoonfuls (leveled) of the Third Reagent. recap securely and shake vigorously for 5 seconds.
6. Remove black cap from reaction bottle and recap securely using the turret cap within 20 seconds.
7. Start the timer and wait for 10 minutes.
8. After waiting 10 minutes, pull the turret up. Carefully remove the test strip with the testing pad. Use to color chart and match the color of the exposed side of the testing pad within the next 2 minutes.
9. Record your result.

A.3.2 Hach

Materials: Hach's EZ Arsenic Test Kits
Methodology:

1. Insert a test strip into the cap so the pad completely covers the small opening. Close the flap and press to secure.
2. Fill the reaction bottle with sample to the fill line (50 mL).
3. Add one Reagent #1 and one Reagent #2 powder pillow to the sample.
4. Immediately attach the cap to the reaction bottle. Swirl continuously for 60 seconds. Do not shake or invert or allow sample to get on the strip.
5. Wait 20 minutes. Swirl twice during the reaction period.
6. Remove the test strip and immediately compare the developed color to the chart on the test strip bottle (0–500 µg/L
7. row). Read strips in the shade.